Baryon-baryon interactions from lattice QCD

Michael Wagman

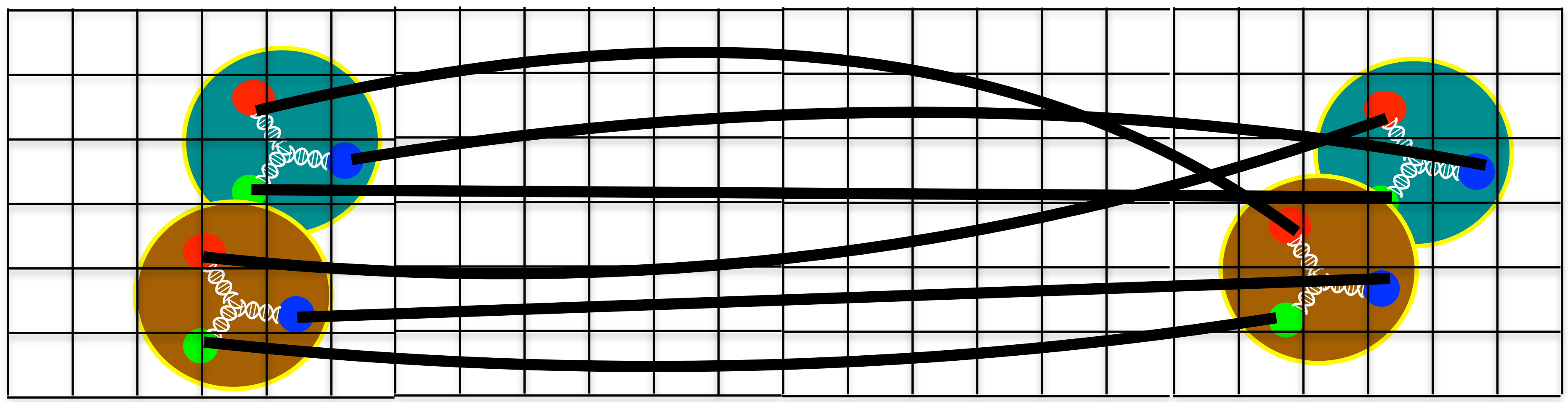

MW, Winter, Chang, Davoudi, Detmold, Orginos, Savage, Shanahan
[NPLQCD], PRD 96 (2017) arXiv:1706.06550

Elba 2019

Lepton interactions with
nucleons and nuclei

The Standard Model

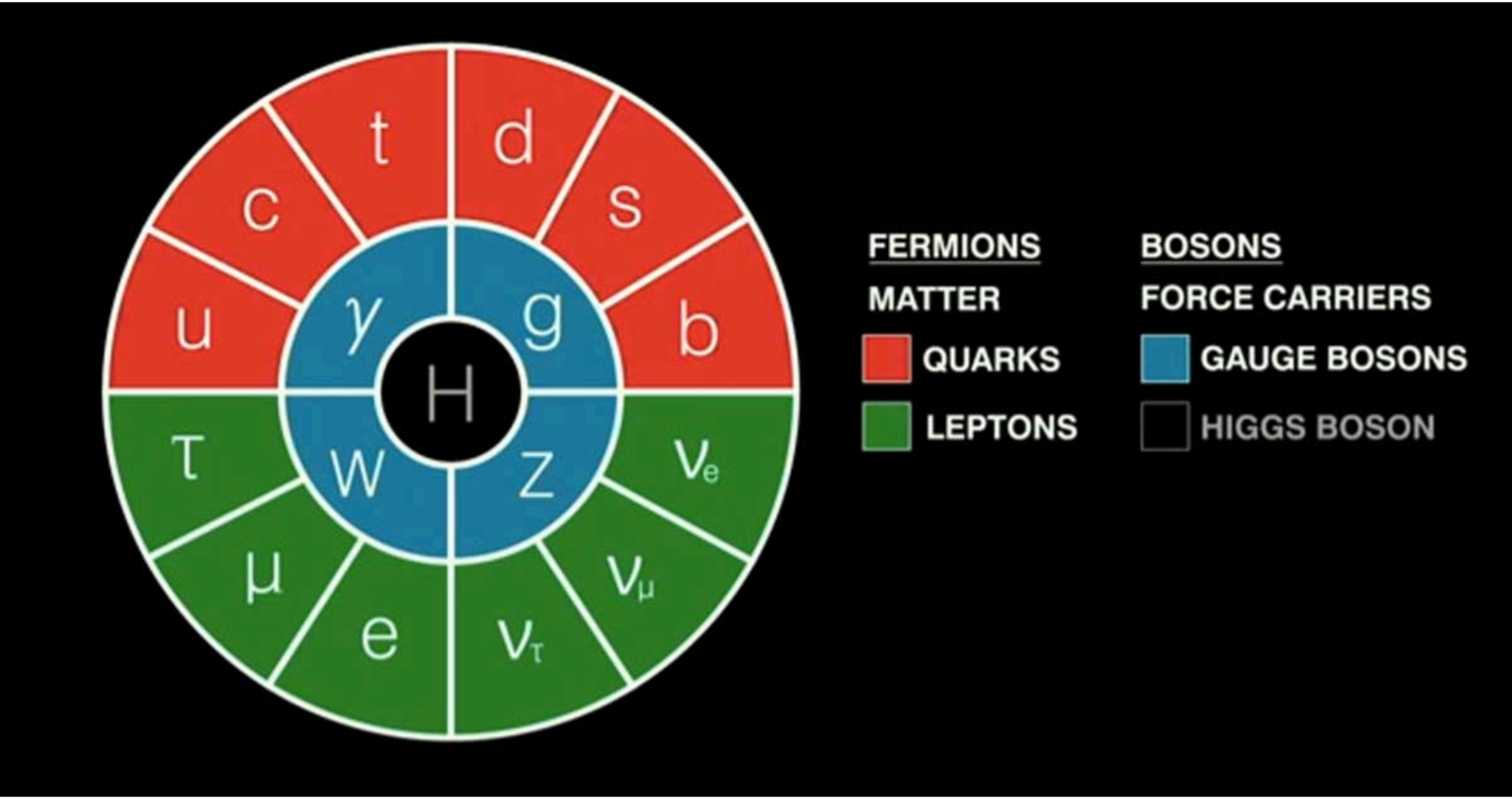

The Standard Model

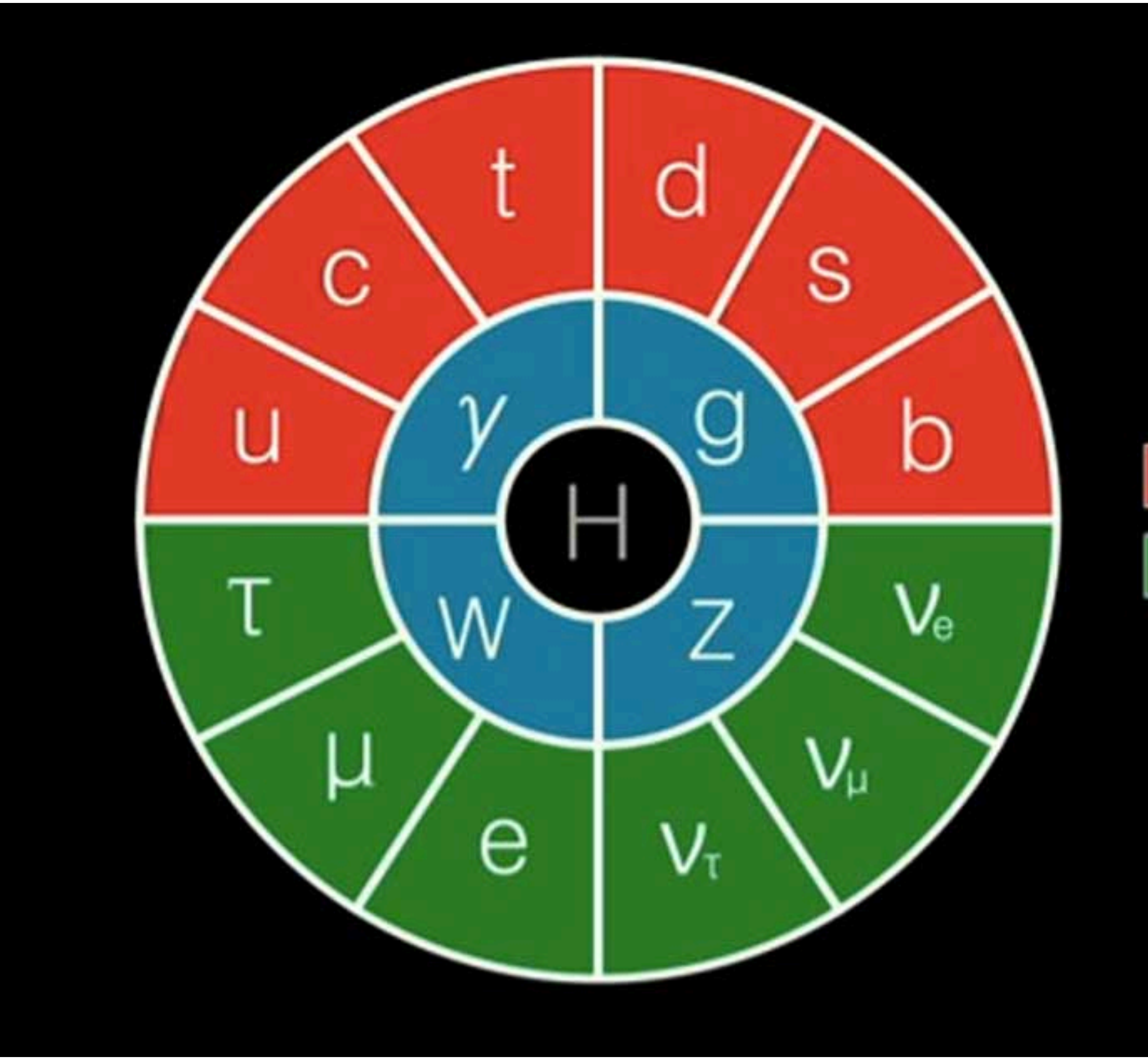

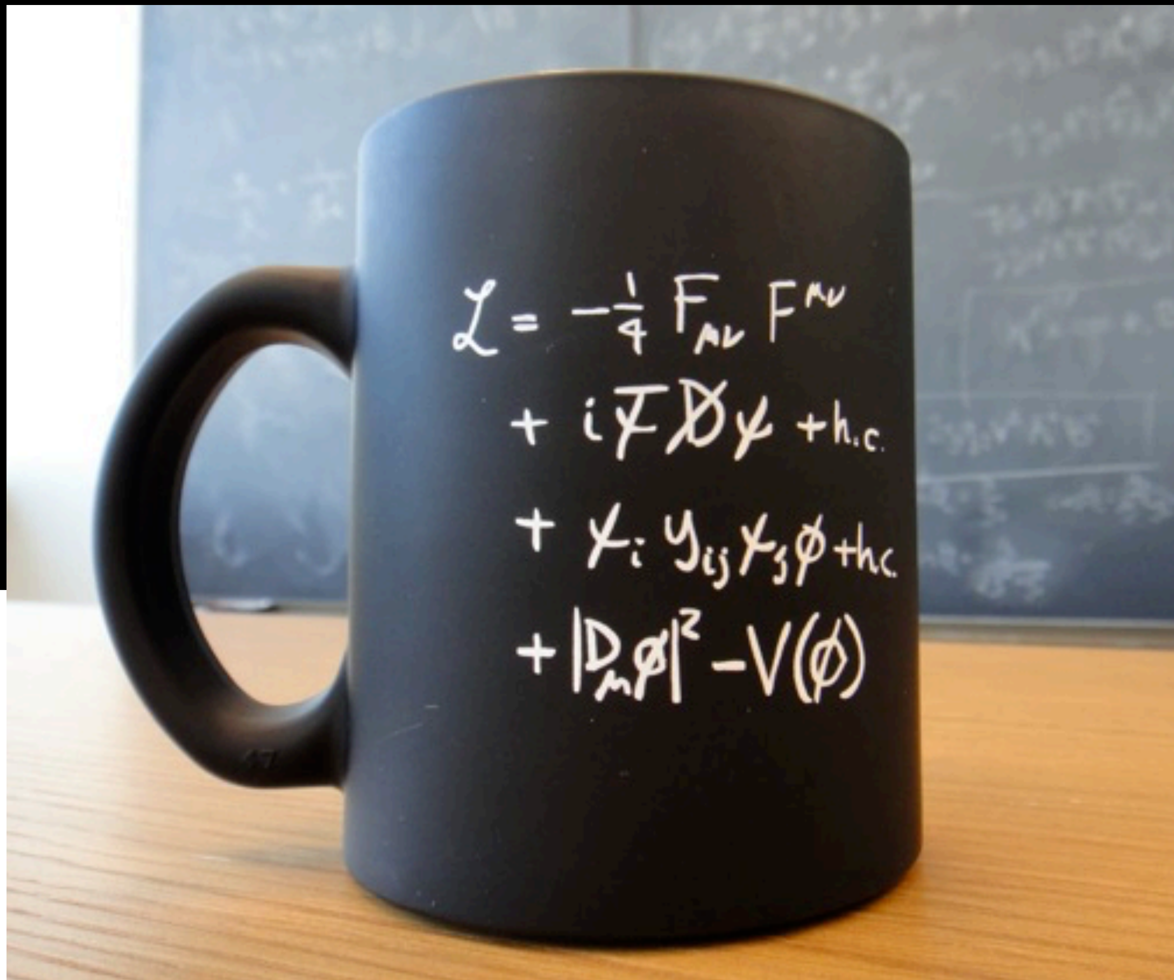

Emergent complexity

Can baryon-baryon interactions be understood from the Standard Model?

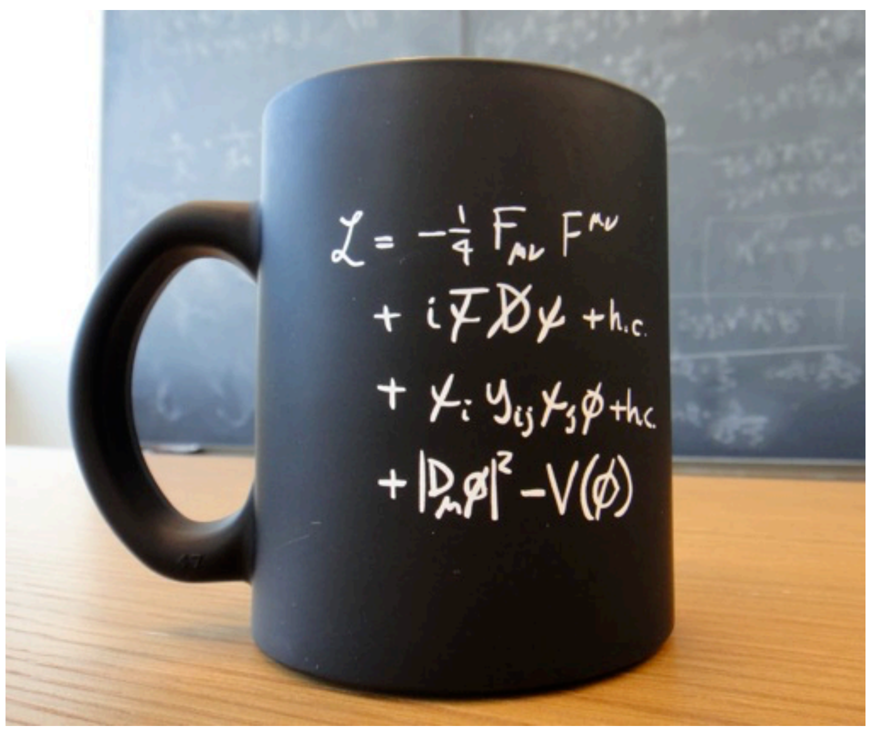

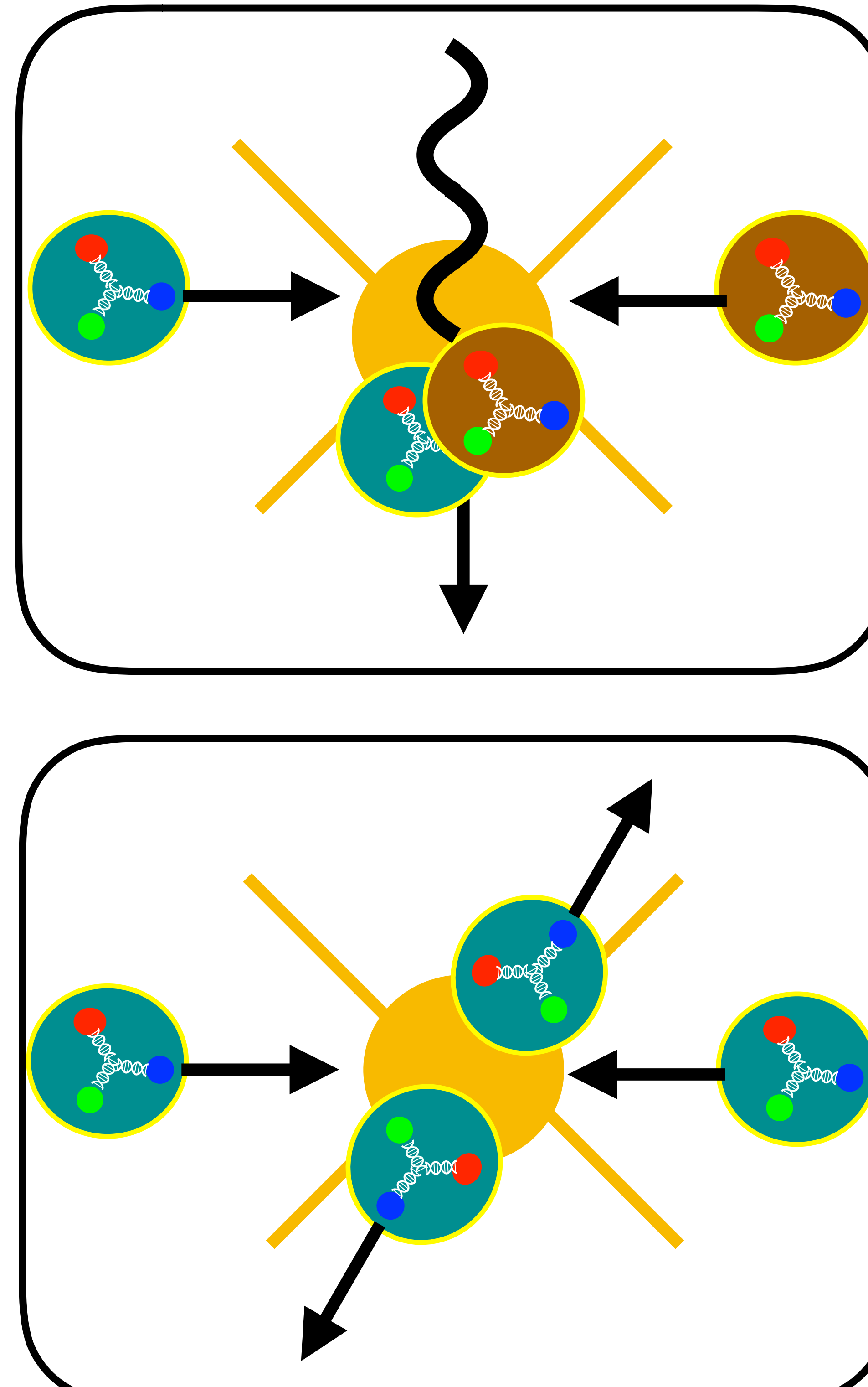

Lattice QCD

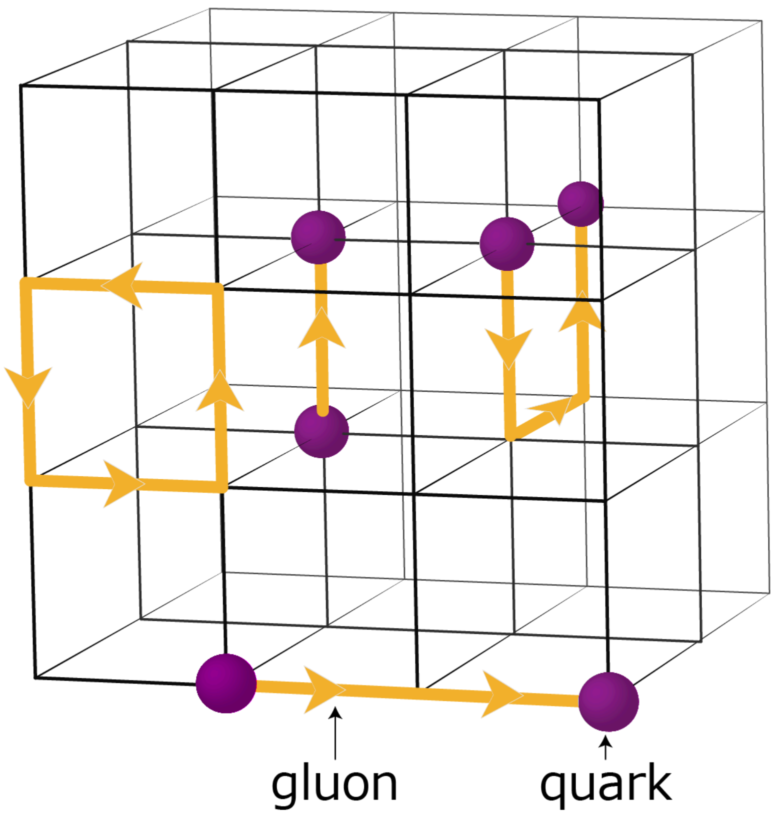

Approximating spacetime as a discrete lattice with a finite size makes QCD path integrals finite

$$\langle \mathcal{O} \rangle = Z^{-1} \int \mathcal{D}U \mathcal{D}\overline{q} \mathcal{D}q \; e^{-S_{QCD}(U,q,\overline{q})} \mathcal{O}(U,q,\overline{q})$$

$$= Z^{-1} \int \mathcal{D}U \; e^{-S_g(U)} \det(\not{D}(U) + m_q) \; \mathcal{O}(U, [\not{D}(U) + m_q]^{-1})$$

Lattice action defines an EFT for QCD valid at lengths larger than lattice scale

QCD properties of hadrons reproduced by LQCD up to lattice cutoff artifacts removed by continuum extrapolation

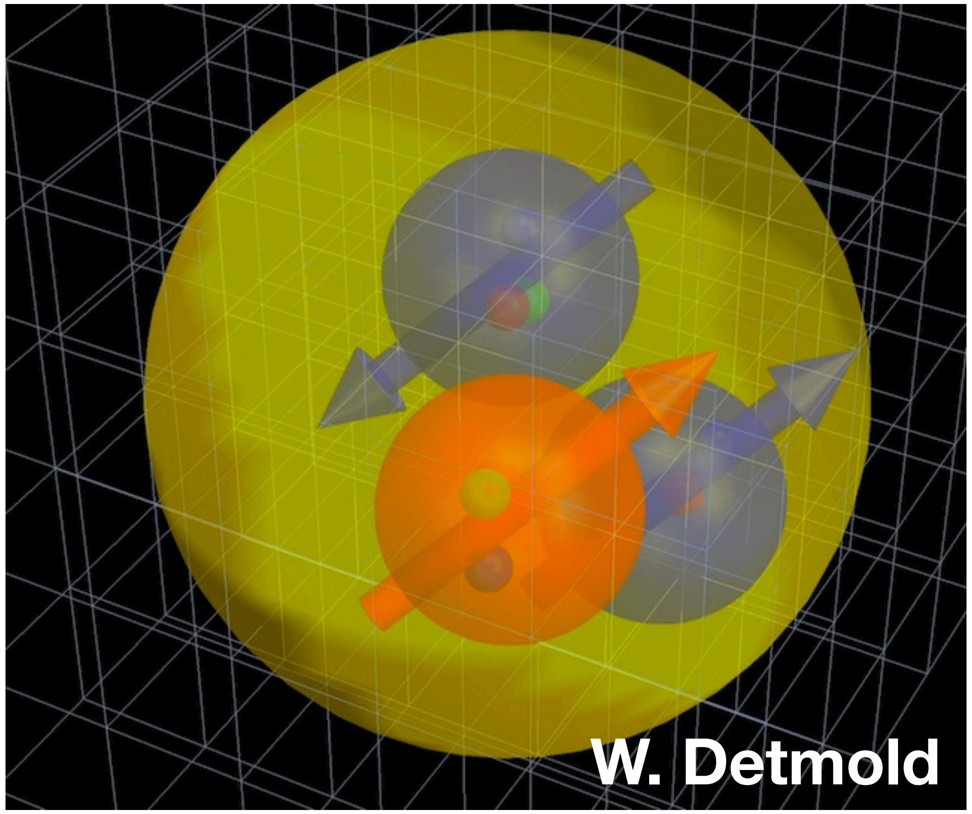

Building baryons

Generic products of quark and gluon fields act as **interpolating operators** with some overlap onto all QCD eigenstates with right quantum numbers

$$\mathcal{O}(q,\overline{q},U)\,|0\rangle = \sum_{n=0}^{N_{max}} Z_n\,|n\rangle \qquad\qquad e^{-H_{QCD}}\,|n\rangle = e^{-E_n}\,|n\rangle$$

Simple choice: point-like product of quark fields projected to color-singlet, positive-parity, definite spin*

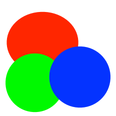

$$B_P^{\pm}(x) = \varepsilon_{ijk}\left[q_i^{+}(x)q_j^{-}(x) - q_i^{-}(x)q_j^{+}(x)\right]q_k^{\pm}(x) \qquad q_i^{\pm}(x) = \left(\frac{1+\gamma_4}{2}\right)(1 \pm i\gamma_3\gamma_5)q(x)$$

Better ground-state overlap: build baryons from quark fields "smeared" over spatial region over radius $\sim 1\ \mathrm{fm}$

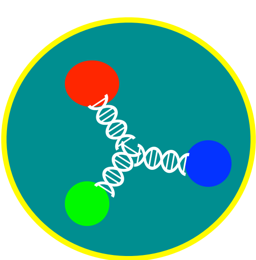

$$B_S^{\pm}(x):\ \ q(x) \to S[q(x)] \qquad S[q_i^{\pm}(\mathbf{x},t)] = \int d^3\mathbf{y}\ S_{ij}(\mathbf{x},\mathbf{y})q_j^{\pm}(\mathbf{y},t)$$

* spacetime symmetry broken to hypercubic subgroup

Operators classified by hypercubic irreps, $B^{\pm} \sim G_{1g}$

See e.g. Basak et al [LHPC] PRD 72 (2005)

Baryon correlation functions

Energy spectrum of QCD extracted from baryon correlation functions

— products of creation/annihilation operators separated in Euclidean time

$$G^{\pm}_{SS}(t, \mathbf{p}) =$$

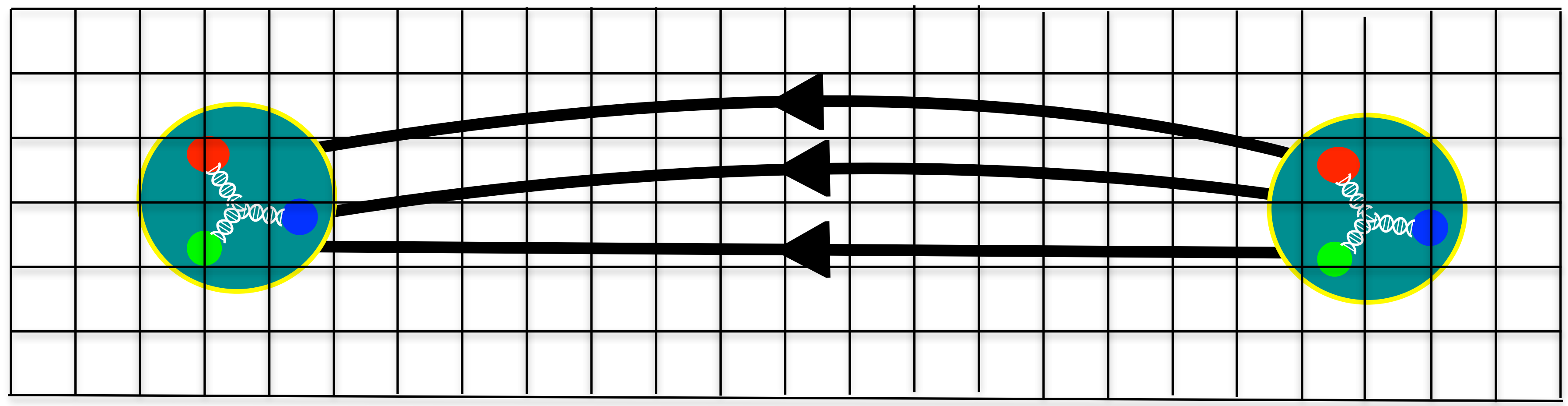

G has **spectral representation**

$$G^{\pm}_{SS}(t,\mathbf{p}) \approx \langle 0| \, B^{\pm}_{S}(\mathbf{p},t) B^{\pm}_{S}(0)^{\dagger} \, |0\rangle$$

$$= \sum_n \langle 0| \, e^{H_{QCD}t} B^{\pm}_{S}(\mathbf{p},0) e^{-H_{QCD}t} \, |n\rangle \, \langle n| \, B^{\pm}_{S}(0)^{\dagger} \, |0\rangle$$

$$= \sum_n e^{-E_n t} \left| \langle 0| \, B^{\pm}_{S}(0) \, |n,\mathbf{p}\rangle \right|^2 \equiv \sum_n \left| Z^S_n \right|^2 e^{-E_n t}$$

Baryon mass determined by fitting G at large t to sum of few exponentials

Two baryons

Baryon-baryon correlation functions can be built from momentum-projected baryons

$$G_{SS}^{3S1,+}(t,\mathbf{d},\mathbf{k}) = \sum_{\mathbf{x},\mathbf{y}} e^{i\left(\frac{2\pi}{L}\right)\mathbf{d}\cdot(\mathbf{x}+\mathbf{y})} e^{i\frac{\mathbf{k}}{2}\cdot(\mathbf{x}-\mathbf{y})} \left\langle B_S^{+}(\mathbf{x},t) B_S^{+}(\mathbf{y},t) B_S^{+}(0)^{\dagger} B_S^{+}(0)^{\dagger} \right\rangle$$

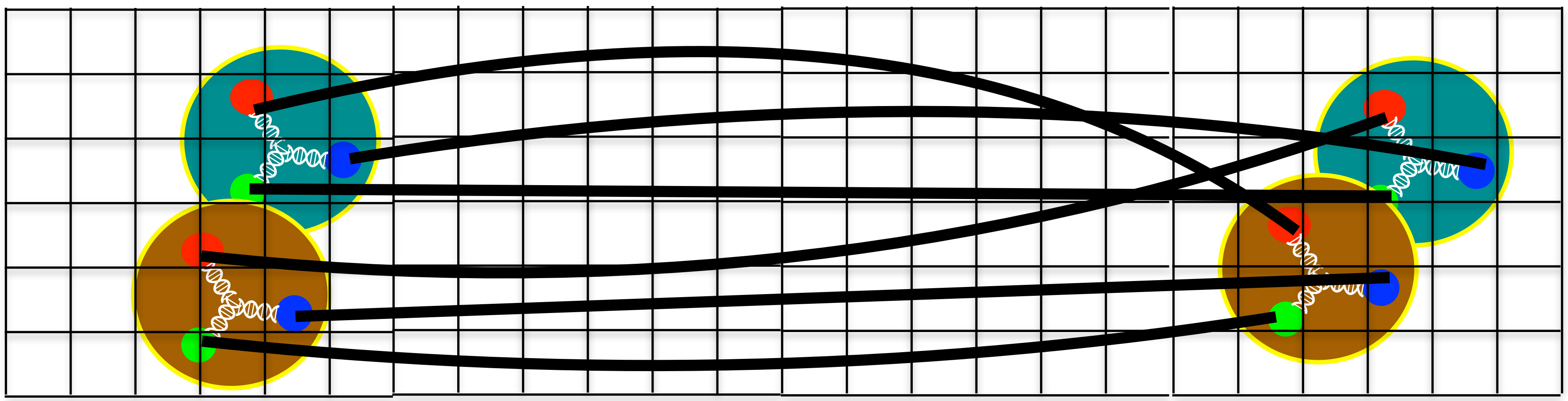

Wick contractions can be performed efficiently in terms of baryon blocks, see

Detmold, Orginos, PRD 87 (2013)   Doi, Endres, Comput. Phys. Commun. 184 (2013)

$\mathbf{k} = 0$ → Expect high overlap with ground-state of loosely bound nucleus

$\mathbf{k} \neq 0$ → Expect high overlap with baryon-baryon scattering states

Assumption: states with different $\mathbf{k}$ *are orthogonal*

Relaxing this requires variational operator basis, work in progress

Correlation functions give finite-volume energies of bound/“scattering” states

Finite-volume hadron interactions

Volume scaling of energy levels allows bound and scattering states to be distinguished using finite-volume Euclidean information

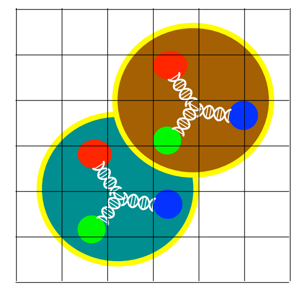

Infinite-volume scattering state

$$[E(L) - E(\infty)] \propto \frac{a}{ML^3}$$

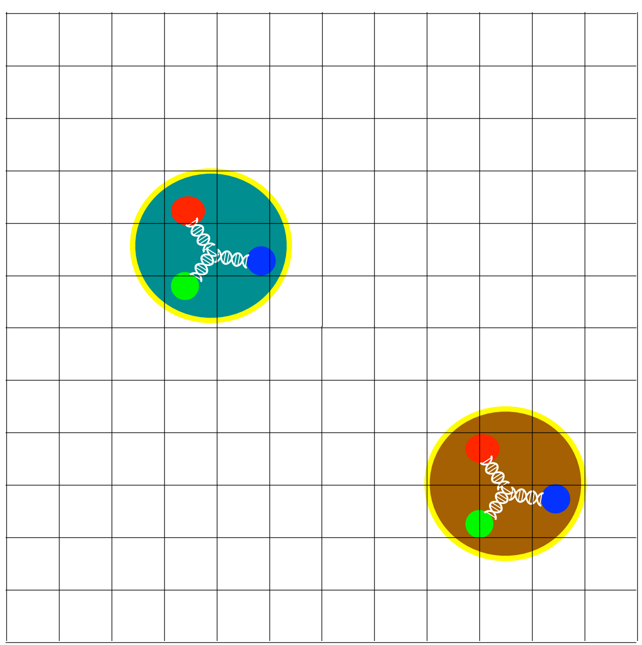

Infinite-volume bound state

$$[E(L) - E(\infty)] \propto \frac{e^{-\gamma L}}{L}$$

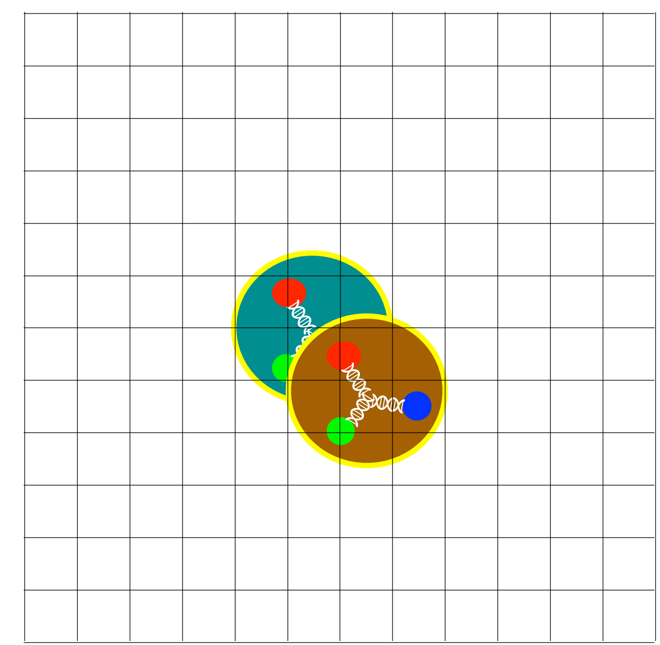

Quantitative information about interactions encoded in volume dependence

Lüscher, Commun. Math. Phys. 105 (1986)

Huang, Yang, Phys. Rev. 105 (1957)

Beane et al, Phys. Lett. B 585 (2004)

Lüscher methods

Quantization condition for energy levels of 2-particle system in a box generically

$$\det\left[F^{-1} + \mathcal{M}\right] = 0$$

Fixed by geometry of box, mixes infinite tower of partial waves

Desired scattering amplitude

Recent review: Briceño, Dudek, Young, Rev. Mod. Phys. 90 (2018)

Interested only in *s*-wave scattering (physical *d*-wave component of deuteron higher order in EFT), neglect mixing between $\ell = 0$ and $\ell = 4$, equal masses

Simplified QC: $$k^* \cot\delta(k^*) = \frac{1}{\pi L \gamma} \sum_{\mathbf{n}\in\mathbb{Z}^3} \frac{1}{\left(\hat{\gamma}^{-1}(\mathbf{n} - \frac{1}{2}\mathbf{d})\right)^2 - \left(\frac{k^* L}{2\pi}\right)^2}$$

With center-of-mass energy and momentum and usual relativistic γ factor,

$$E^{*2} = E^2 - \left(\frac{2\pi}{L}\mathbf{d}\right)^2 \qquad k^* = \frac{1}{2}\sqrt{E^{*2} - 4M_B^2} \qquad \gamma = \frac{E}{E^*}$$

Each finite-volume energy level gives us one constraint on δ at a particular k^*

The signal-to-noise problem

Monte Carlo noise in (multi-)baryon correlation functions grows exponentially with Euclidean time separation

Correlation function variance can be analyzed as a correlation function

Parisi, Phys. Rept. 103 (1984) Lepage, Boulder TASI (1989)

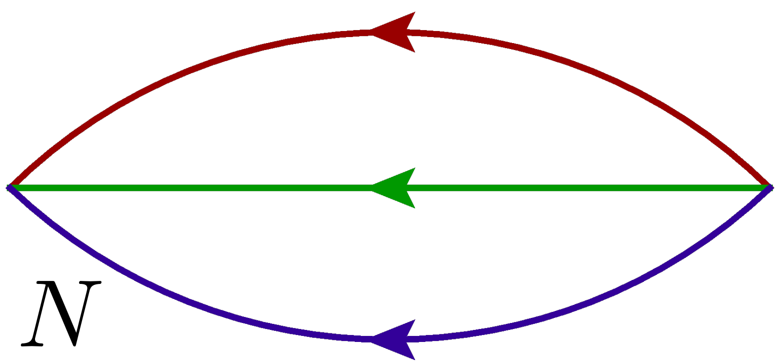

$$G_N \sim e^{-M_N t}$$

$$\mathrm{Var}(G_N) \sim \left\langle \left| N(t) N(0)^\dagger \right| \right\rangle$$

$$\sim e^{-3 m_\pi t}$$

$$\frac{G_N}{\sqrt{\mathrm{Var}(G_N)}} \sim e^{-\left(M_N - \frac{3}{2} m_\pi\right) t}$$

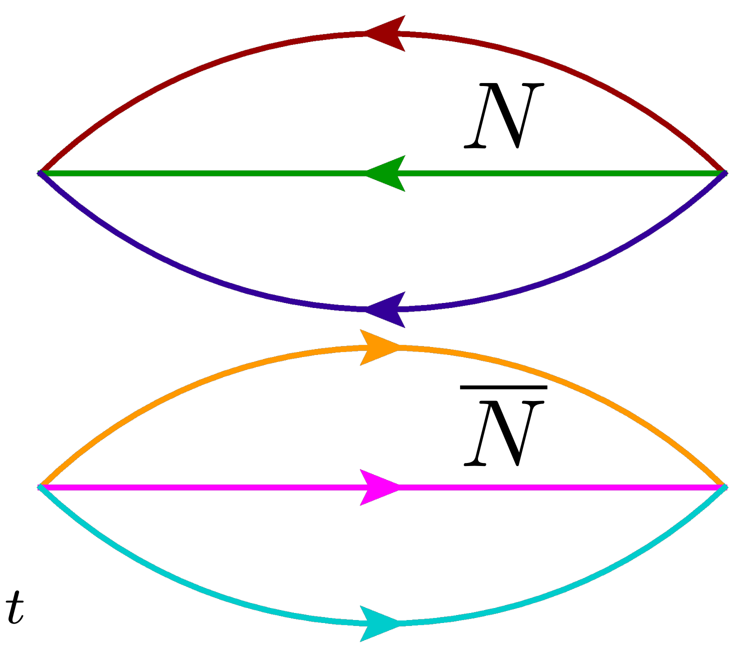

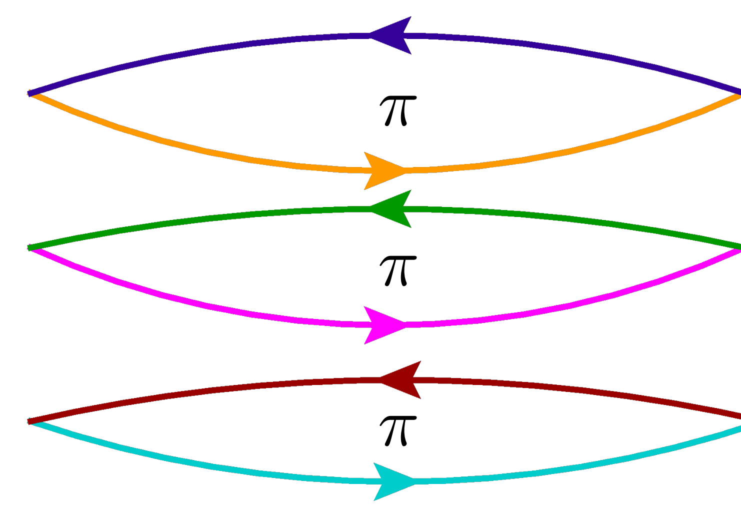

Multi-nucleon: $\sim e^{-A\left(M_N - \frac{3}{2} m_\pi\right) t}$

Noise equivalently arises from phase fluctuations of operators charged under $U_1(B)$, solving noise problem requires solving “sign problem” MW, Savage, PRD 96 (2017)

Changing the quark masses

$m_\pi \sim 140$ MeV

$m_\pi \sim 800$ MeV

Nucleon effective mass: $M_N(t) = -\partial_t \ln G_N(t) = M_N + O\left(e^{-(E_1 - M_N)t}\right)$

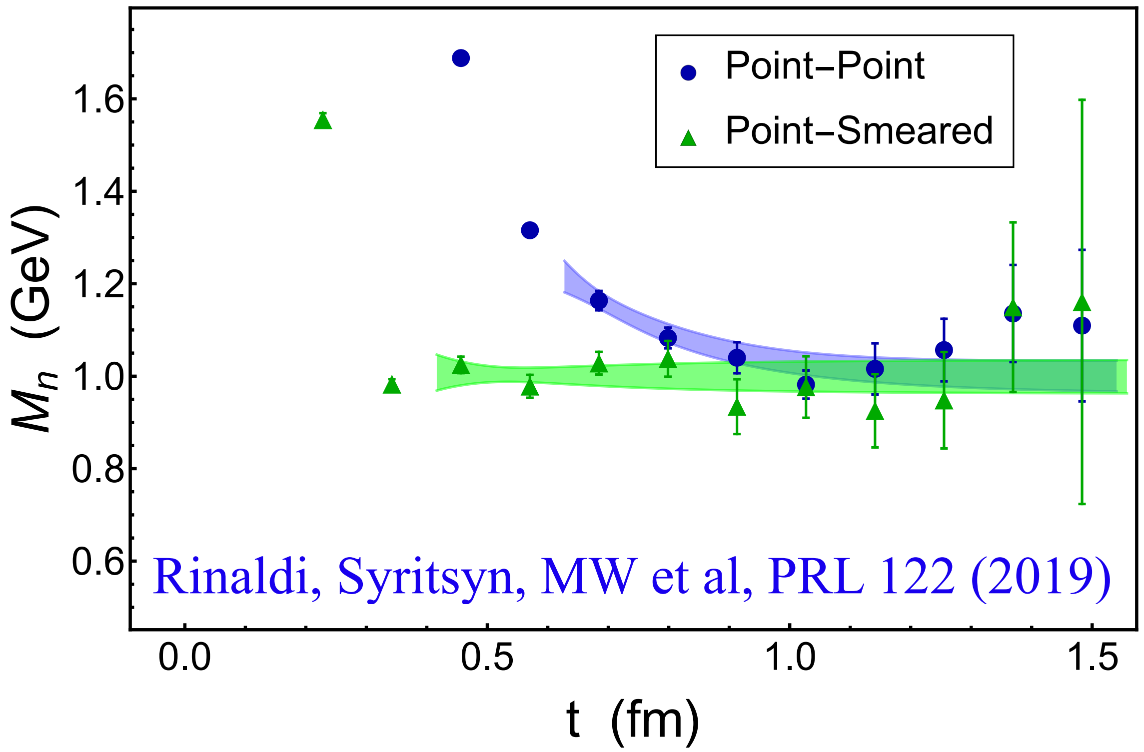

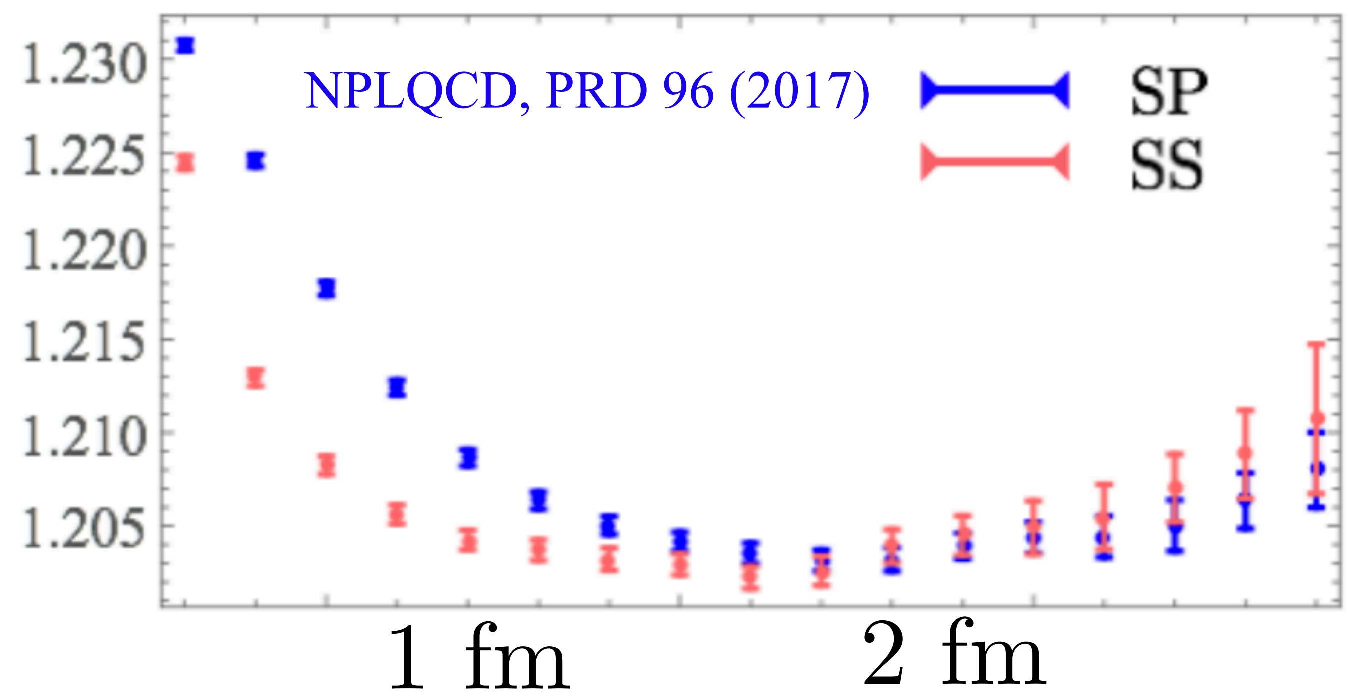

$$M_N \sim \frac{3}{2}m_\pi + \left(M_N - \frac{3}{2}m_\pi\right)$$

$$M_N \sim 210 \text{ MeV} + 730 \text{ MeV}$$

$$\frac{\mathrm{Var}[G_{BB}(t = 1 \text{ fm})]}{\mathrm{Var}[G_{BB}(t=0)]} \sim \frac{2,600,000}{N_{meas}}$$

$$M_N \sim 1200 \text{ MeV} + 400 \text{ MeV}$$

$$\frac{\mathrm{Var}[G_{BB}(t = 1 \text{ fm})]}{\mathrm{Var}[G_{BB}(t=0)]} \sim \frac{3,300}{N_{meas}}$$

Two baryons in a box

$SU(3)$ flavor symmetric world with *u* and *d* degenerate with physical *s* quark explored by NPLQCD

$$N_f = 3,\ m_\pi = 806(9)\ \text{MeV},\ a = 0.145(2)\ \text{fm}$$

NPLQCD, PRD 87 (2013) NPLQCD, PRD 96 (2017)
NPLQCD, PRC 88 (2013) …

Baryon-baryon scattering channels can be classified into $SU(3)$ irreps

$$8 \otimes 8 = 27 \oplus 10 \oplus \overline{10} \oplus 8_S \oplus 8_A \oplus 1$$

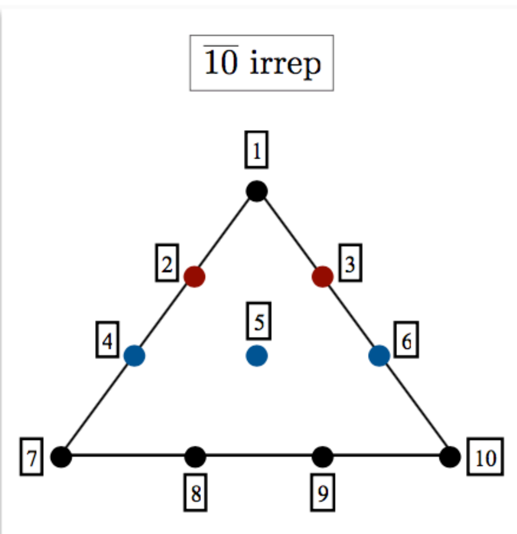

	Flavor channel
1	$\frac{1}{\sqrt{2}}(pn - np)$
2	$-\sqrt{\frac{1}{3}}\Sigma^0 n + \sqrt{\frac{2}{3}}\Sigma^- p / \Lambda n$
3	$\sqrt{\frac{2}{3}}\Sigma^+ n + \sqrt{\frac{1}{3}}\Sigma^0 p / \Lambda p$
4	$\frac{1}{\sqrt{2}}(\Sigma^-\Sigma^0 - \Sigma^0\Sigma^-)/\Xi^- n/\Lambda\Sigma^-$
5	$\frac{1}{\sqrt{2}}(\Sigma^-\Sigma^+ - \Sigma^+\Sigma^-)/\frac{1}{\sqrt{2}}(\Xi^- p - \Xi^0 n)/\Lambda\Sigma^0$
6	$\frac{1}{\sqrt{2}}(\Sigma^0\Sigma^+ - \Sigma^+\Sigma^0)/\Xi^0 p/\Lambda\Sigma^+$
7	$\Sigma^-\Xi^-$
8	$-\sqrt{\frac{2}{3}}\Sigma^0\Xi^- + \sqrt{\frac{1}{3}}\Sigma^-\Xi^0$
9	$\sqrt{\frac{1}{3}}\Sigma^+\Xi^- + \sqrt{\frac{2}{3}}\Sigma^0\Xi^0$
10	$\Sigma^+\Xi^0$

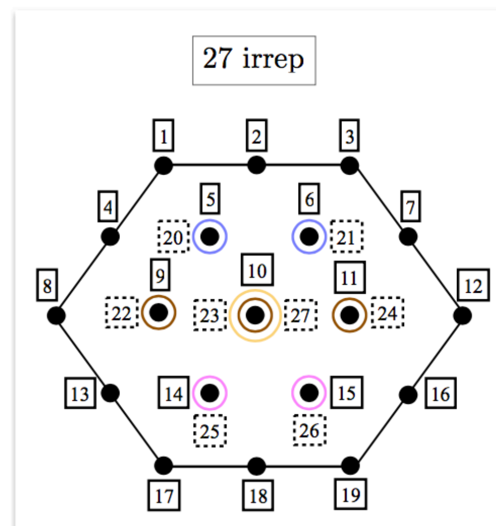

	Flavor channel		Flavor channel
1	nn	14	$-\sqrt{\frac{2}{3}}\Sigma^0\Xi^- + \sqrt{\frac{1}{3}}\Sigma^-\Xi^0$
2	$\frac{1}{\sqrt{2}}(np + pn)$	15	$\sqrt{\frac{1}{3}}\Sigma^+\Xi^- + \sqrt{\frac{2}{3}}\Sigma^0\Xi^0$
3	pp	16	$\Sigma^+\Xi^0$
4	$\Sigma^- n$	17	$\Xi^-\Xi^-$
5	$\sqrt{\frac{2}{3}}\Sigma^0 n + \sqrt{\frac{1}{3}}\Sigma^- p$	18	$\frac{1}{\sqrt{2}}(\Xi^-\Xi^0 + \Xi^0\Xi^-)$
6	$-\sqrt{\frac{1}{3}}\Sigma^+ n + \sqrt{\frac{2}{3}}\Sigma^0 p$	19	$\Xi^0\Xi^0$
7	$\Sigma^+ p$	20	$\Lambda n / -\sqrt{\frac{1}{3}}\Sigma^0 n + \sqrt{\frac{2}{3}}\Sigma^- p$
8	$\Sigma^-\Sigma^-$	21	$\Lambda p / \sqrt{\frac{2}{3}}\Sigma^+ n + \sqrt{\frac{1}{3}}\Sigma^0 p$
9	$\frac{1}{\sqrt{2}}(\Sigma^-\Sigma^0 + \Sigma^0\Sigma^-)$	22	$\Lambda\Sigma^- / \Xi^- n$
10	$\frac{1}{\sqrt{6}}(\Sigma^-\Sigma^+ - 2\Sigma^0\Sigma^0 + \Sigma^+\Sigma^-)$	23	$\Lambda\Sigma^0 / \frac{1}{\sqrt{2}}(\Xi^- p - \Xi^0 n)$
11	$\frac{1}{\sqrt{2}}(\Sigma^0\Sigma^+ + \Sigma^+\Sigma^0)$	24	$\Lambda\Sigma^+ / \Xi^0 p$
12	$\Sigma^+\Sigma^+$	25	$\Lambda\Xi^- / \sqrt{\frac{1}{3}}\Sigma^0\Xi^- + \sqrt{\frac{2}{3}}\Sigma^-\Xi^0$
13	$\Sigma^-\Xi^-$	26	$\Lambda\Xi^0 / -\sqrt{\frac{2}{3}}\Sigma^+\Xi^- + \sqrt{\frac{1}{3}}\Sigma^0\Xi^0$
27	$\frac{1}{\sqrt{3}}(\Sigma^+\Sigma^- + \Sigma^0\Sigma^0 + \Sigma^-\Sigma^+)/\frac{1}{\sqrt{2}}(\Xi^0 n + \Xi^- p)/\Lambda\Lambda$		

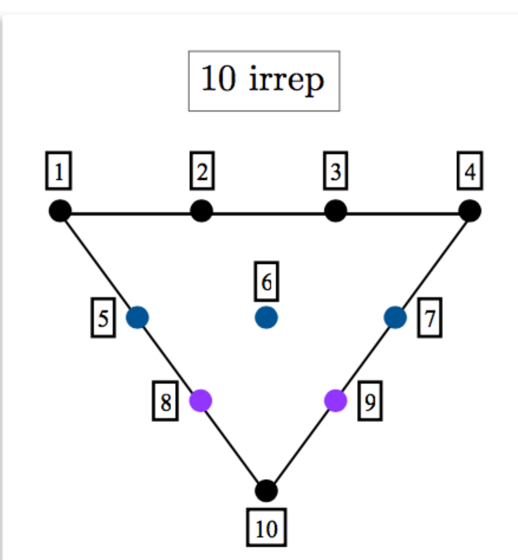

	Flavor channel
1	$\Sigma^- n$
2	$\sqrt{\frac{2}{3}}\Sigma^0 n + \sqrt{\frac{1}{3}}\Sigma^- p$
3	$-\sqrt{\frac{1}{3}}\Sigma^+ n + \sqrt{\frac{2}{3}}\Sigma^0 p$
4	$\Sigma^+ p$
5	$\frac{1}{\sqrt{2}}(\Sigma^-\Sigma^0 - \Sigma^0\Sigma^-)/\Xi^- n/\Lambda\Sigma^-$
6	$\frac{1}{\sqrt{2}}(\Sigma^-\Sigma^+ - \Sigma^+\Sigma^-)/\frac{1}{\sqrt{2}}(\Xi^- p - \Xi^0 n)/\Lambda\Sigma^0$
7	$\frac{1}{\sqrt{2}}(\Sigma^0\Sigma^+ - \Sigma^+\Sigma^0)/\Xi^0 p/\Lambda\Sigma^+$
8	$\sqrt{\frac{1}{3}}\Sigma^0\Xi^- + \sqrt{\frac{2}{3}}\Sigma^-\Xi^0 / \Lambda\Xi^-$
9	$-\sqrt{\frac{2}{3}}\Sigma^+\Xi^- + \sqrt{\frac{1}{3}}\Sigma^0\Xi^0 / \Lambda\Xi^0$
10	$\frac{1}{\sqrt{2}}(\Xi^0\Xi^- - \Xi^-\Xi^0)$

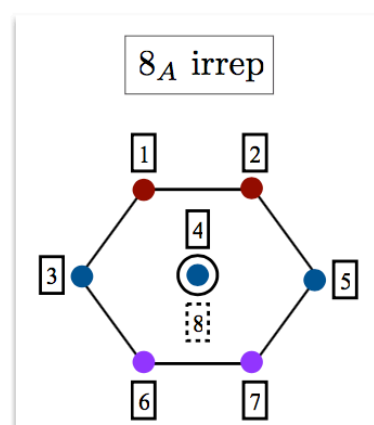

	Flavor channel
1	$-\sqrt{\frac{1}{3}}\Sigma^0 n + \sqrt{\frac{2}{3}}\Sigma^- p / \Lambda n$
2	$\sqrt{\frac{2}{3}}\Sigma^+ n + \sqrt{\frac{1}{3}}\Sigma^0 p / \Lambda p$
3	$\frac{1}{\sqrt{2}}(\Sigma^-\Sigma^0 - \Sigma^0\Sigma^-)/\Xi^- n/\Lambda\Sigma^-$
4	$\frac{1}{\sqrt{2}}(\Sigma^-\Sigma^+ - \Sigma^+\Sigma^-)/\frac{1}{\sqrt{2}}(\Xi^- p - \Xi^0 n)/\Lambda\Sigma^0$
5	$\frac{1}{\sqrt{2}}(\Sigma^0\Sigma^+ - \Sigma^+\Sigma^0)/\Xi^0 p/\Lambda\Sigma^+$
6	$\sqrt{\frac{1}{3}}\Sigma^0\Xi^- + \sqrt{\frac{2}{3}}\Sigma^-\Xi^0 / \Lambda\Xi^-$
7	$-\sqrt{\frac{2}{3}}\Sigma^+\Xi^- + \sqrt{\frac{1}{3}}\Sigma^0\Xi^0 / \Lambda\Xi^0$
8	$\frac{1}{\sqrt{2}}(\Xi^0 n + \Xi^- p)$

$NN\ ^3S_1$

$L^3 \times T = 24^3 \times 48$	$L^3 \times T = 32^3 \times 48$	$L^3 \times T = 48^3 \times 64$
$N_{meas} = 366,912$	$N_{meas} = 219,600$	$N_{meas} = 102,870$

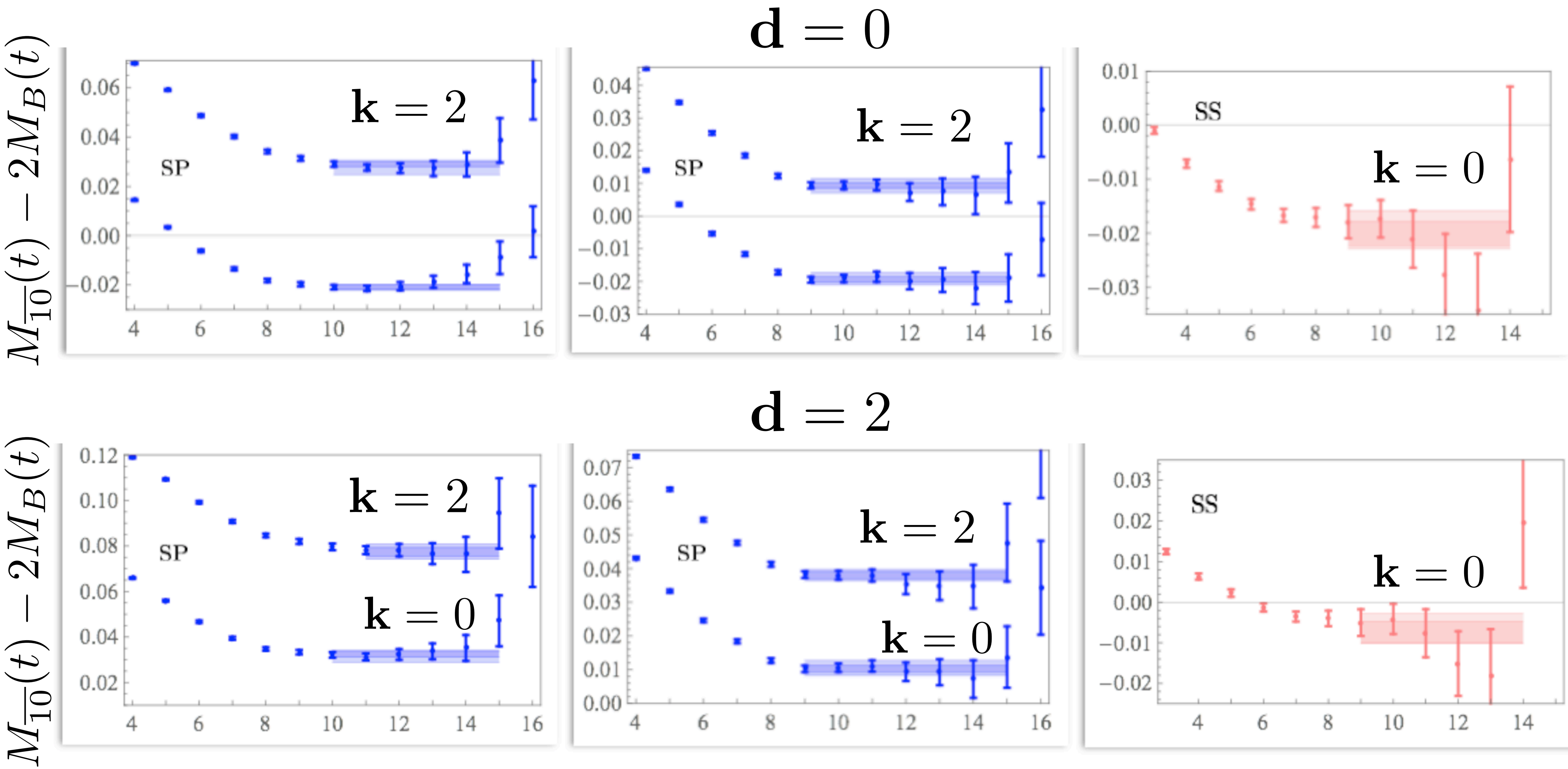

$N_f = 3,\ m_\pi = 806(9)$ MeV, $a = 0.145(2)$ fm

NPLQCD, PRD 96 (2017)

The deuteron

$\mathbf{k} = 0$ correlation functions nearly independent of volume, consistent with infinite-volume bound state

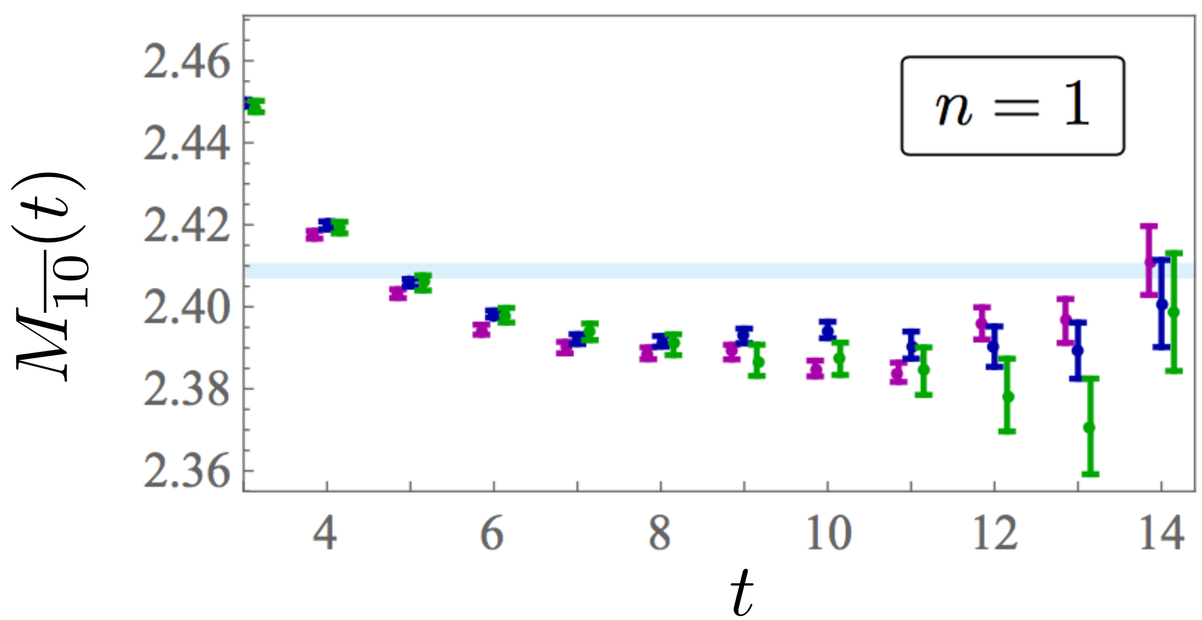

$\mathbf{k} \neq 0$ correlation functions show strong volume dependence consistent with infinite-volume scattering state

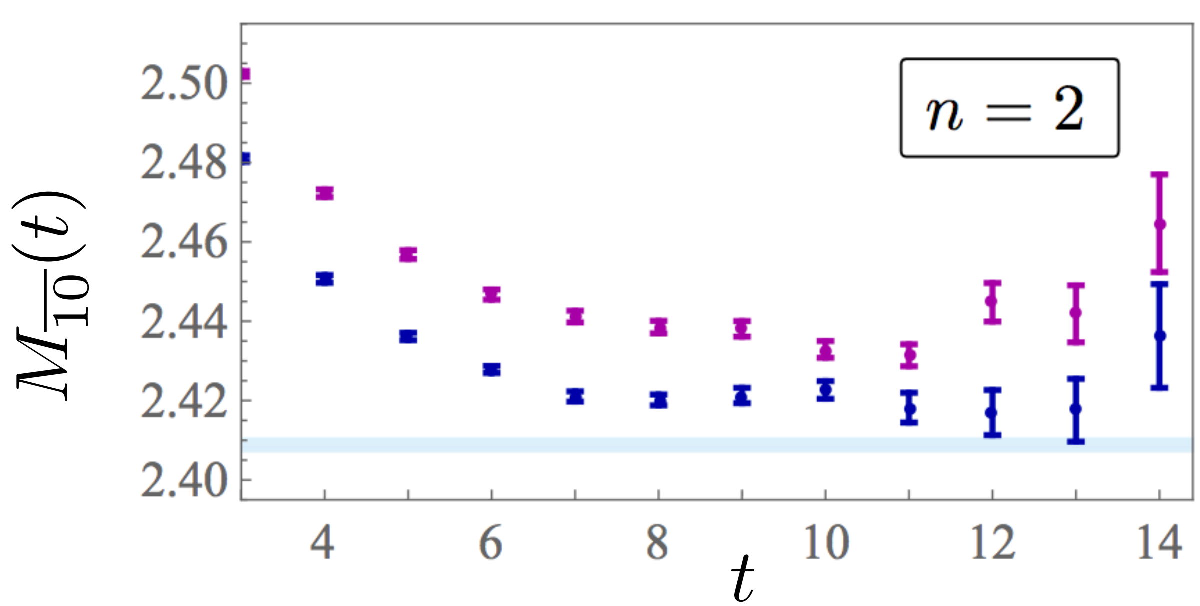

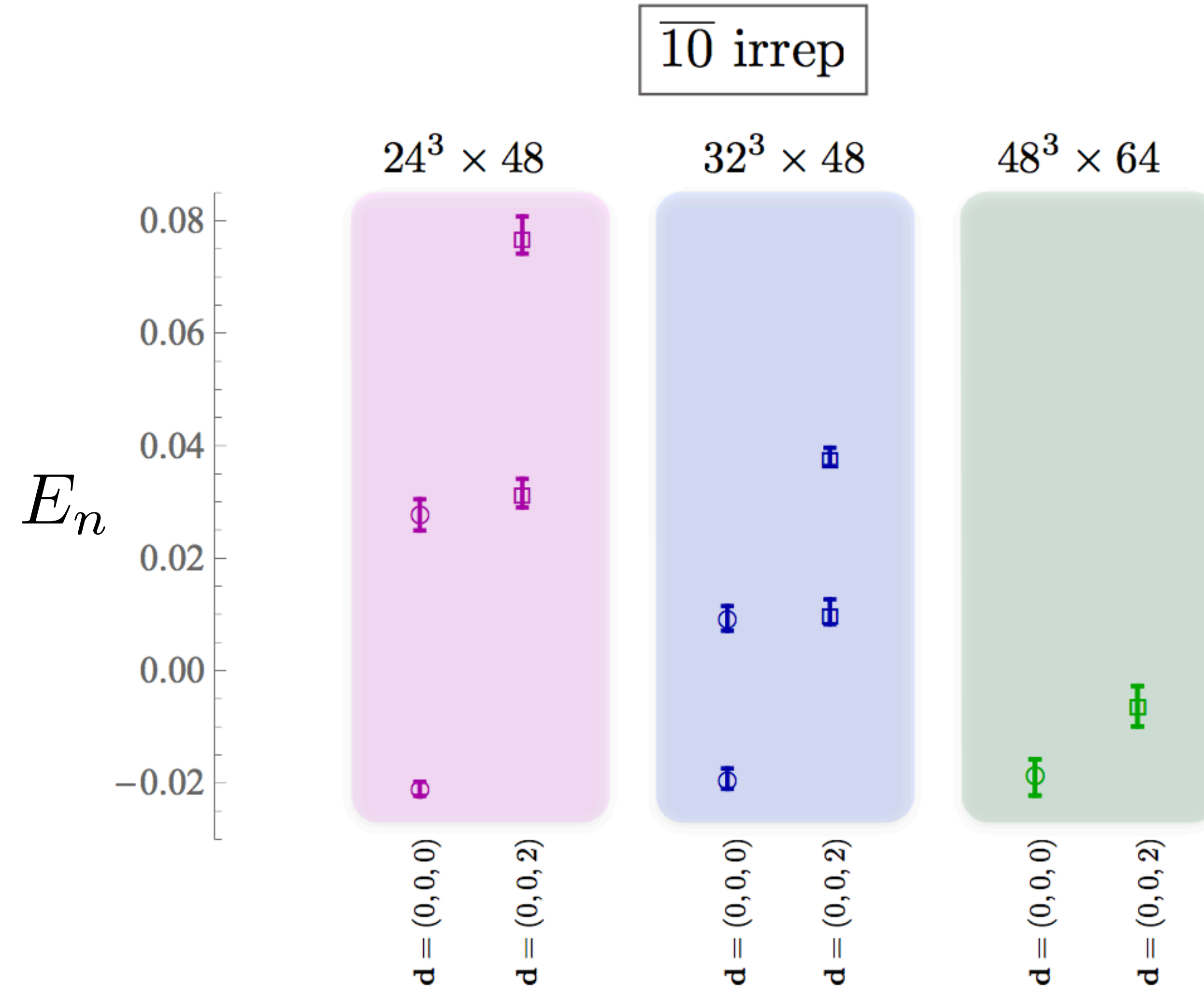

Volume-independence of $\mathbf{k} = 0$ excited state contamination also suggests $\mathbf{k} = 0$ and $\mathbf{k} \neq 0$ dominantly overlap on to different states

$NN\ ^1S_0$: the dineutron

$\mathbf{k} = 0$ correlation functions nearly independent of volume, consistent with infinite-volume bound state

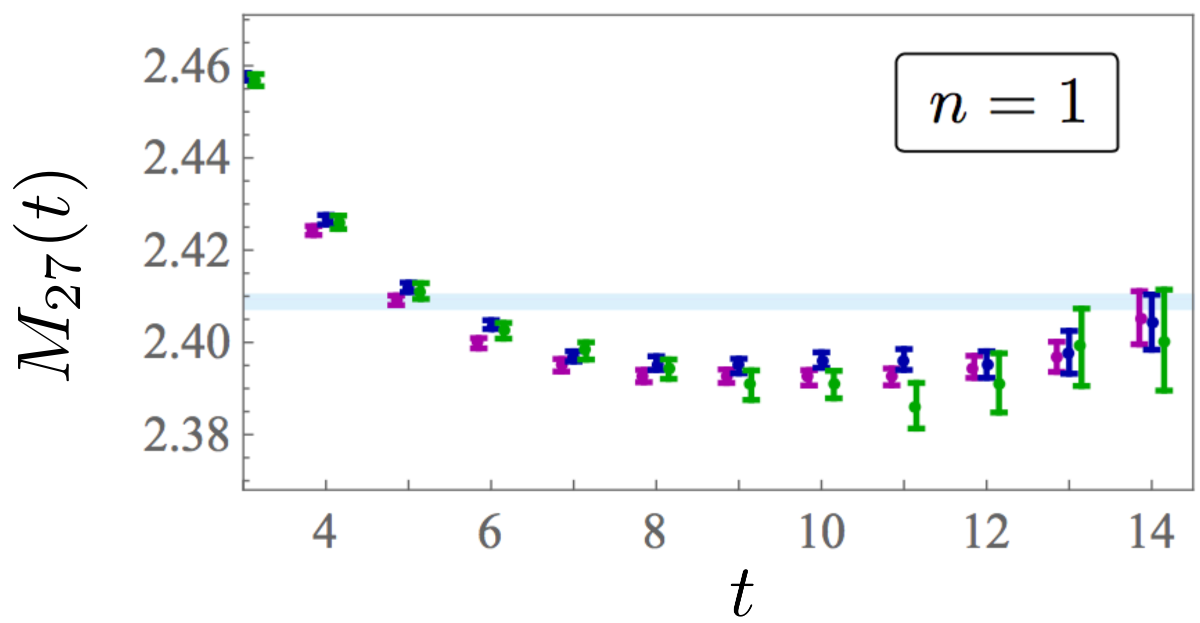

$\mathbf{k} \neq 0$ correlation functions show strong volume dependence consistent with infinite-volume scattering state

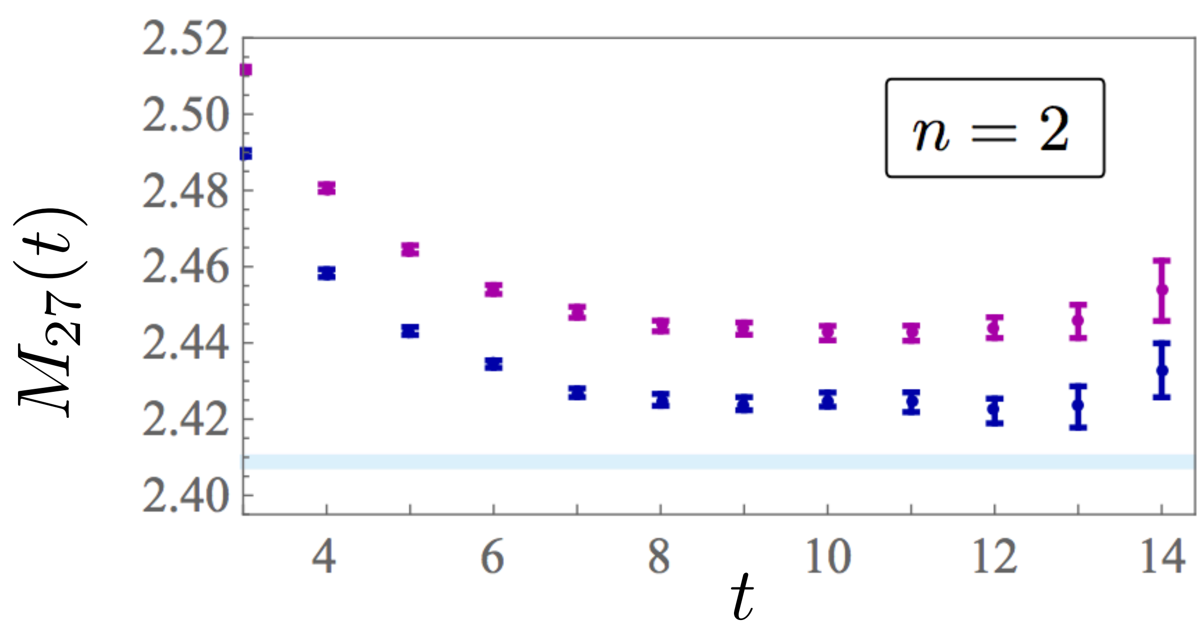

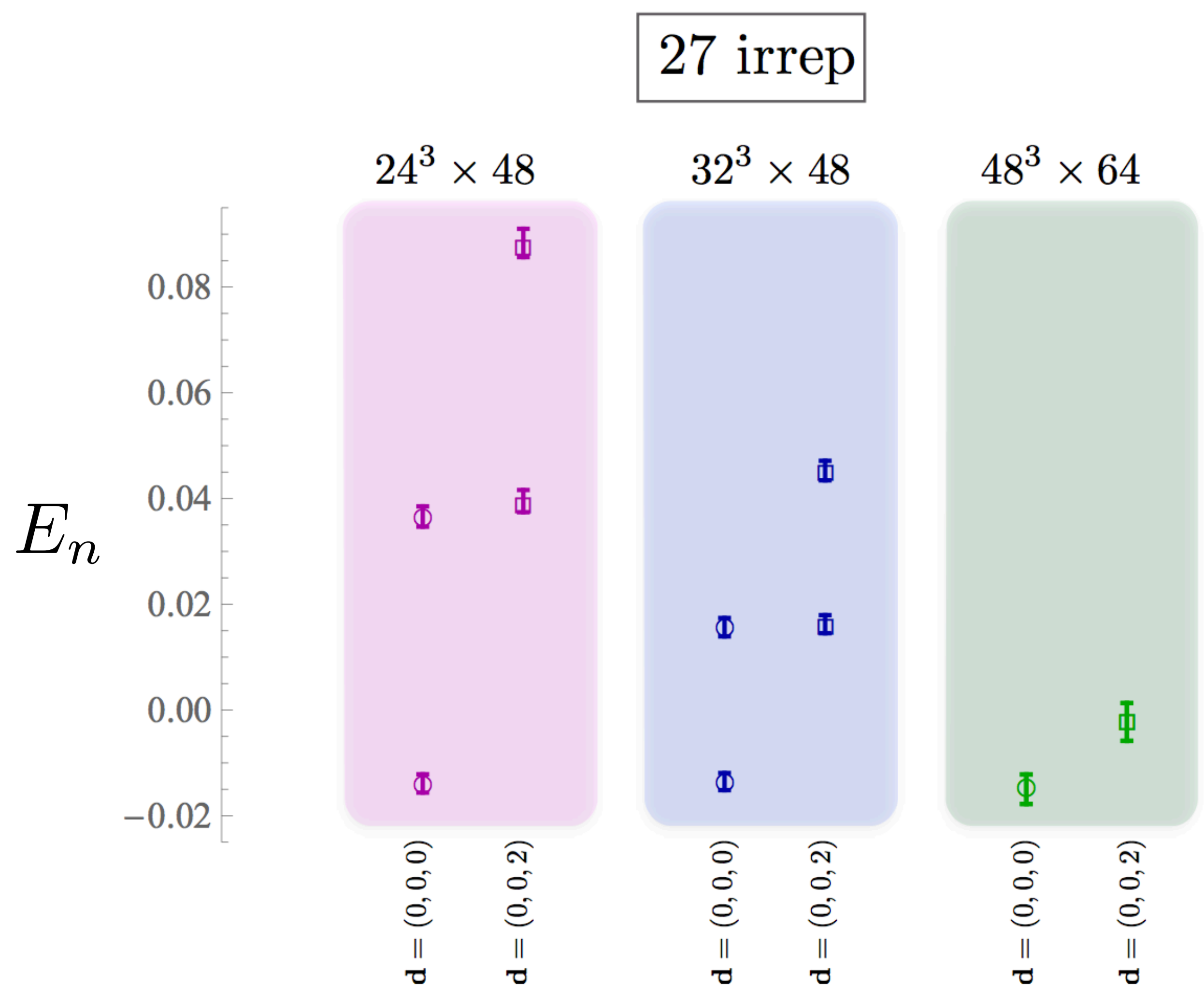

Volume-independence of $\mathbf{k} = 0$ excited state contamination also suggests $\mathbf{k} = 0$ and $\mathbf{k} \neq 0$ dominantly overlap on to different states

$\Xi^0 n + \Xi^- p\ (^3S_1)$

$\mathbf{k} = 0$ correlation functions nearly independent of volume, consistent with infinite-volume bound state

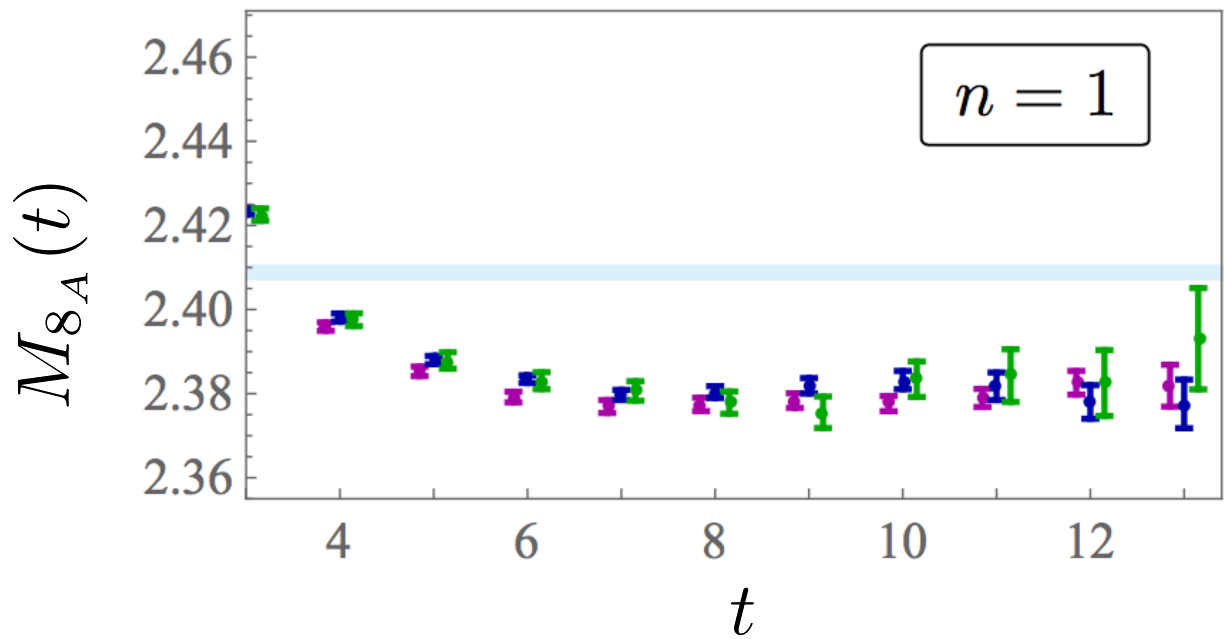

$\mathbf{k} \neq 0$ correlation functions show strong volume dependence consistent with infinite-volume scattering state

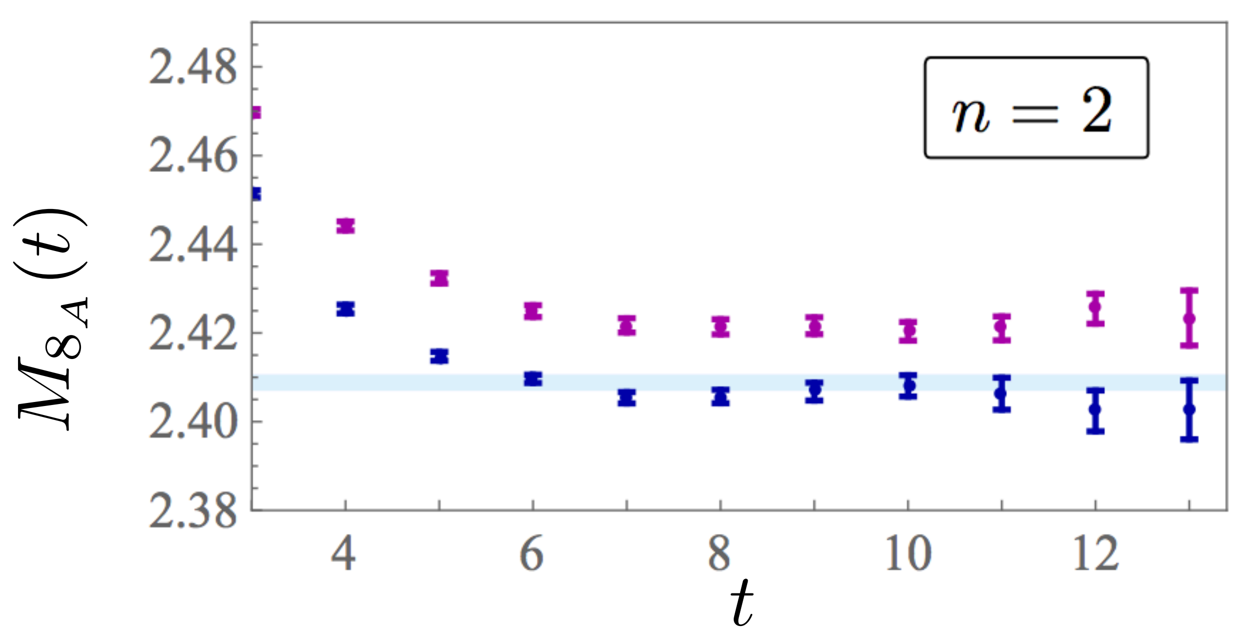

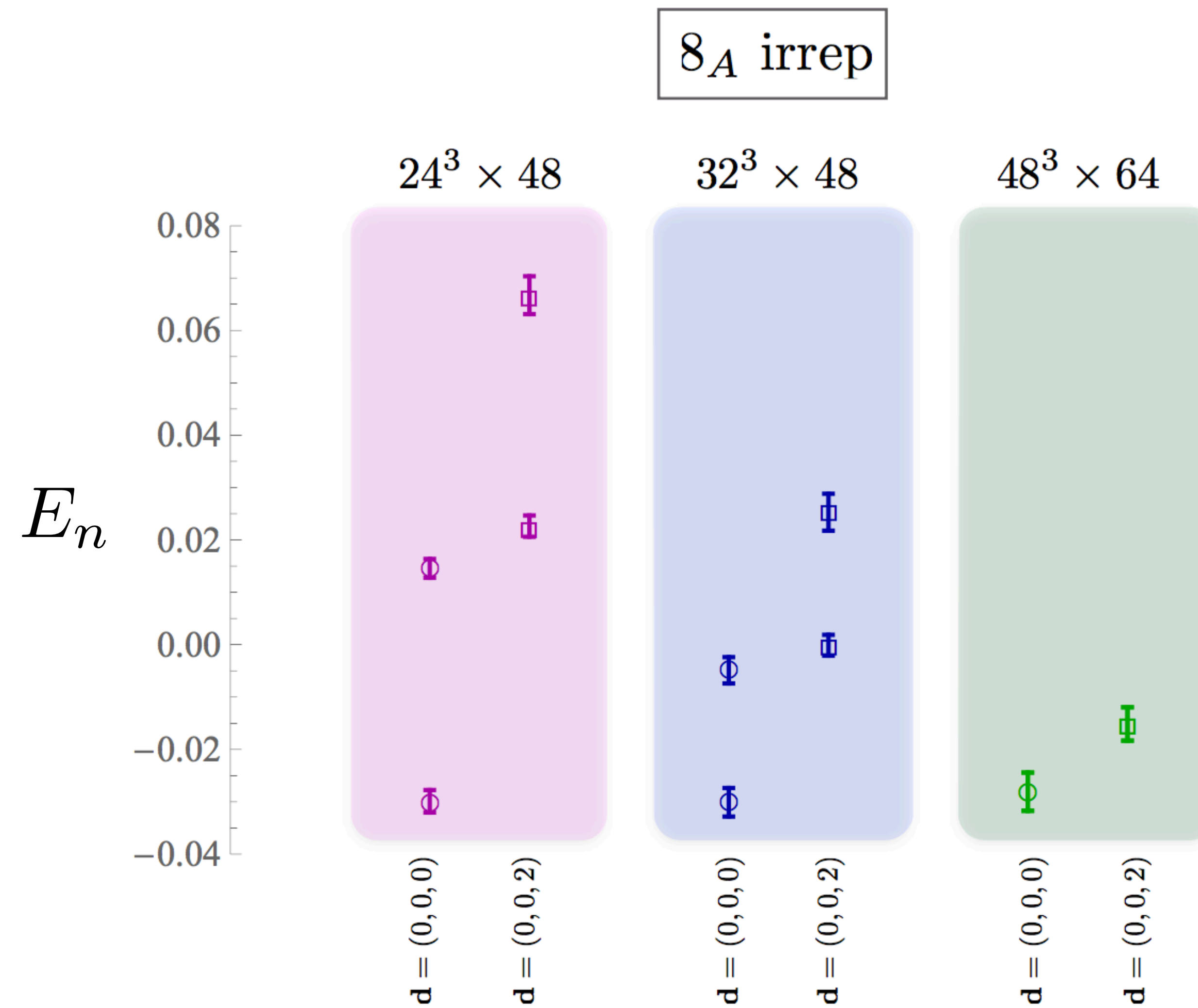

Volume-independence of $\mathbf{k} = 0$ excited state contamination also suggests $\mathbf{k} = 0$ and $\mathbf{k} \neq 0$ dominantly overlap on to different states

$\Sigma^+ p\ (^3S_1)$

$\mathbf{k}=0$ correlation functions consistent with either infinite-volume bound or scattering state

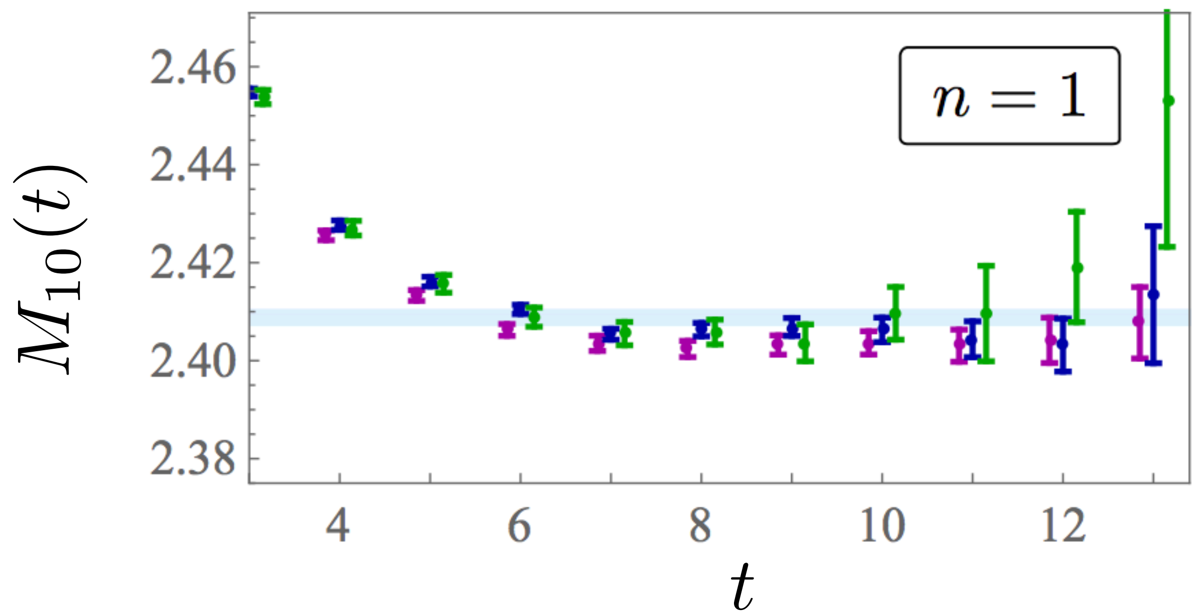

$\mathbf{k}\neq 0$ correlation functions show strong volume dependence consistent with infinite-volume scattering state

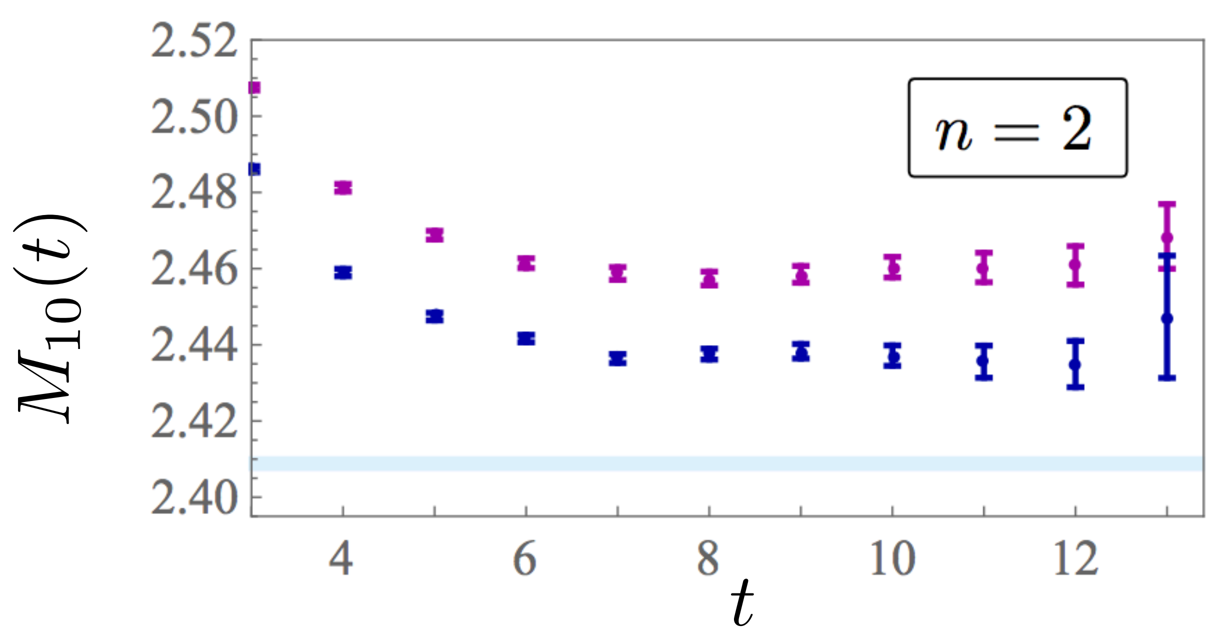

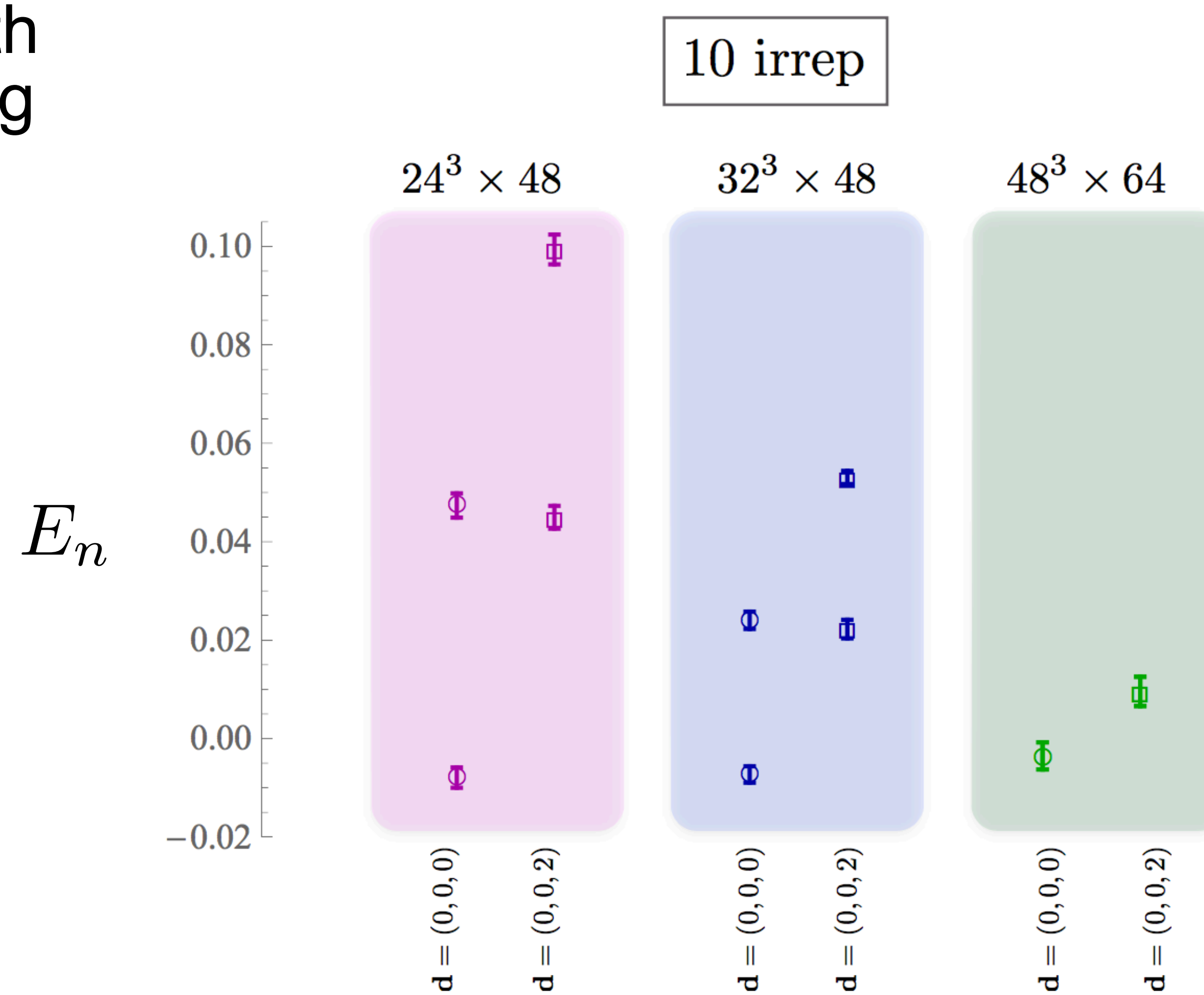

Volume-independence of $\mathbf{k}=0$ excited state contamination also suggests $\mathbf{k}=0$ and $\mathbf{k}\neq 0$ dominantly overlap on to different states

Baryon-baryon phase shifts

10 energy levels for each channel each constrain phase shift at one center-of-mass relative momentum k^* according to Lüscher quantization condition

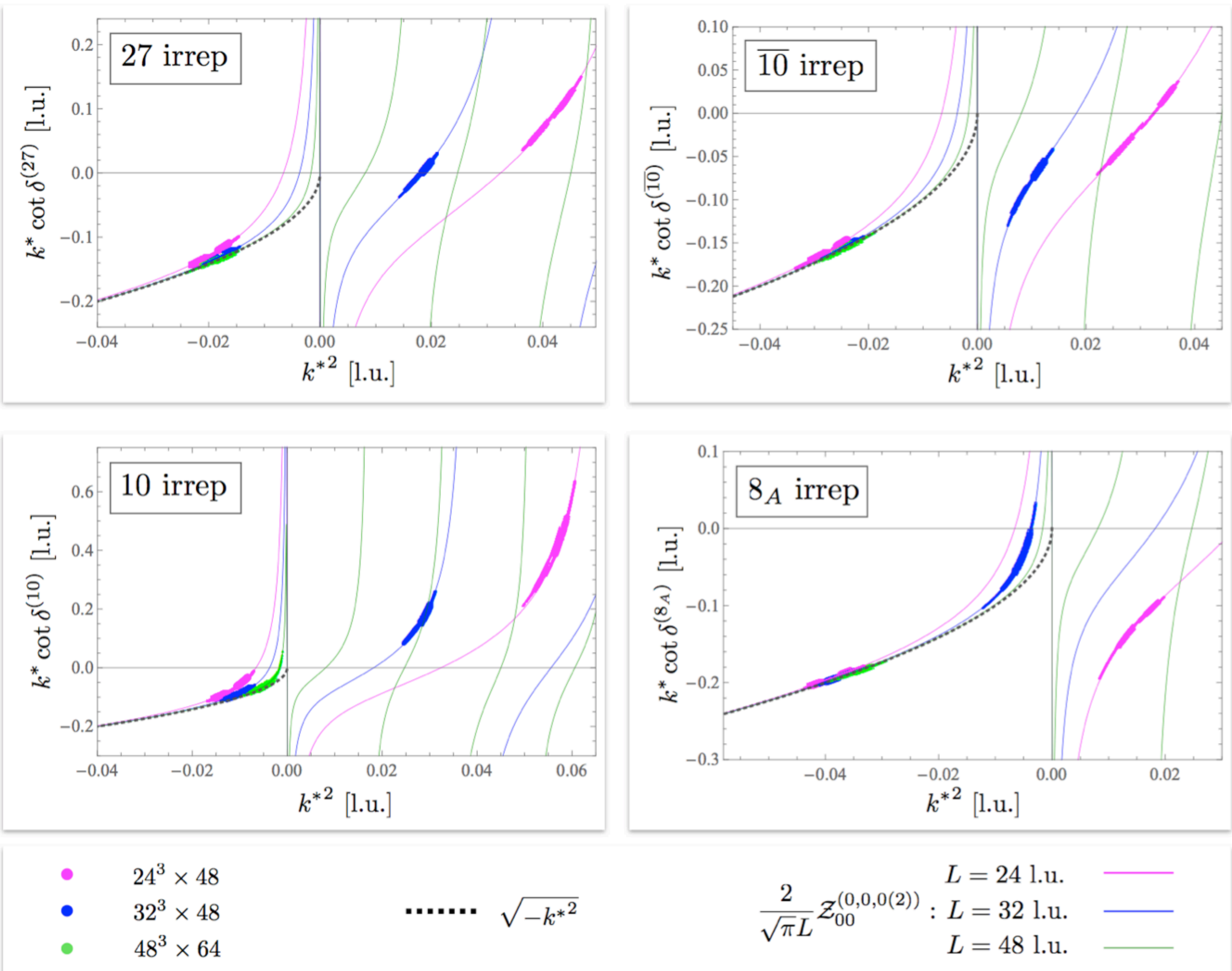

Effective range expansion

All kinematic points where phase shift constrained are below *t* channel cut $k^* = \frac{m_\pi}{2}$

Phase shift should be described by effective range expansion (ERE)

$$k^* \cot\delta(k^*) = -\frac{1}{a} + \frac{1}{2} r k^{*2} + P k^{*4} + \ldots$$

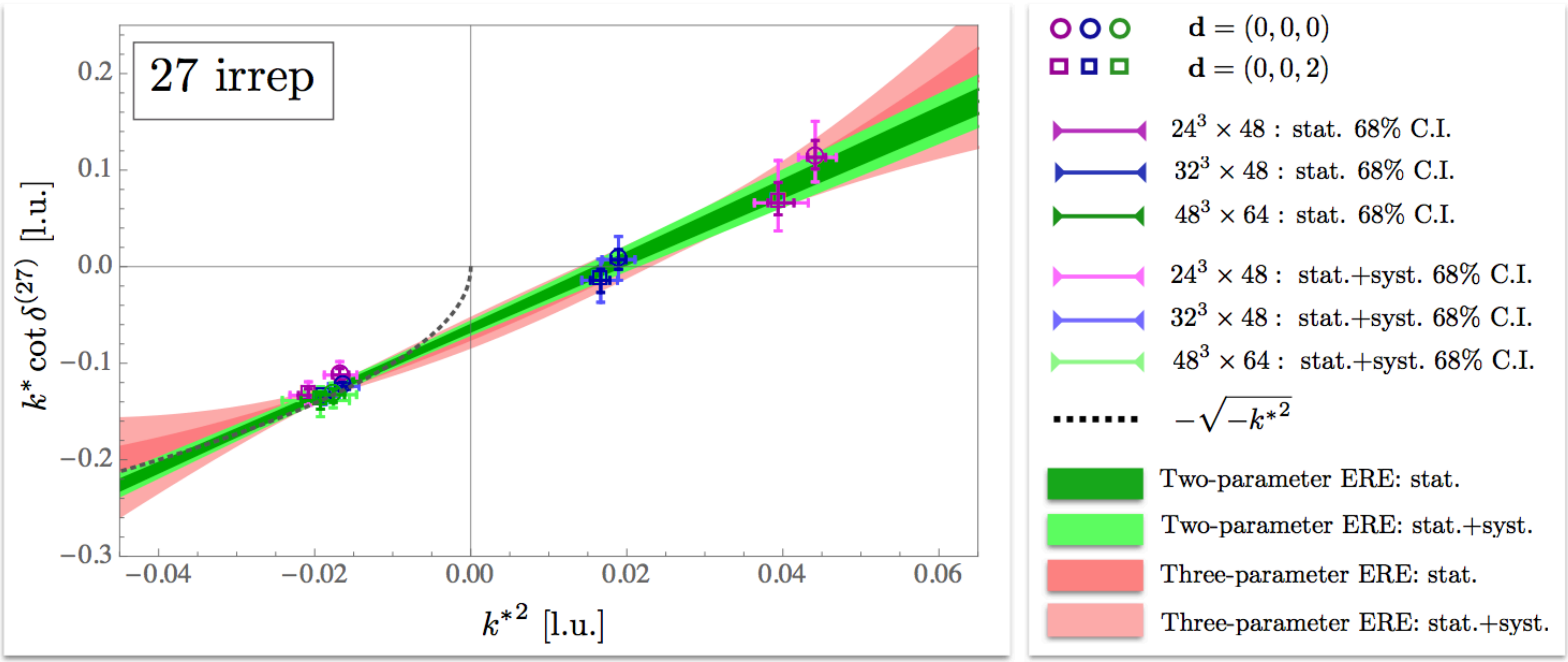

ERE fits

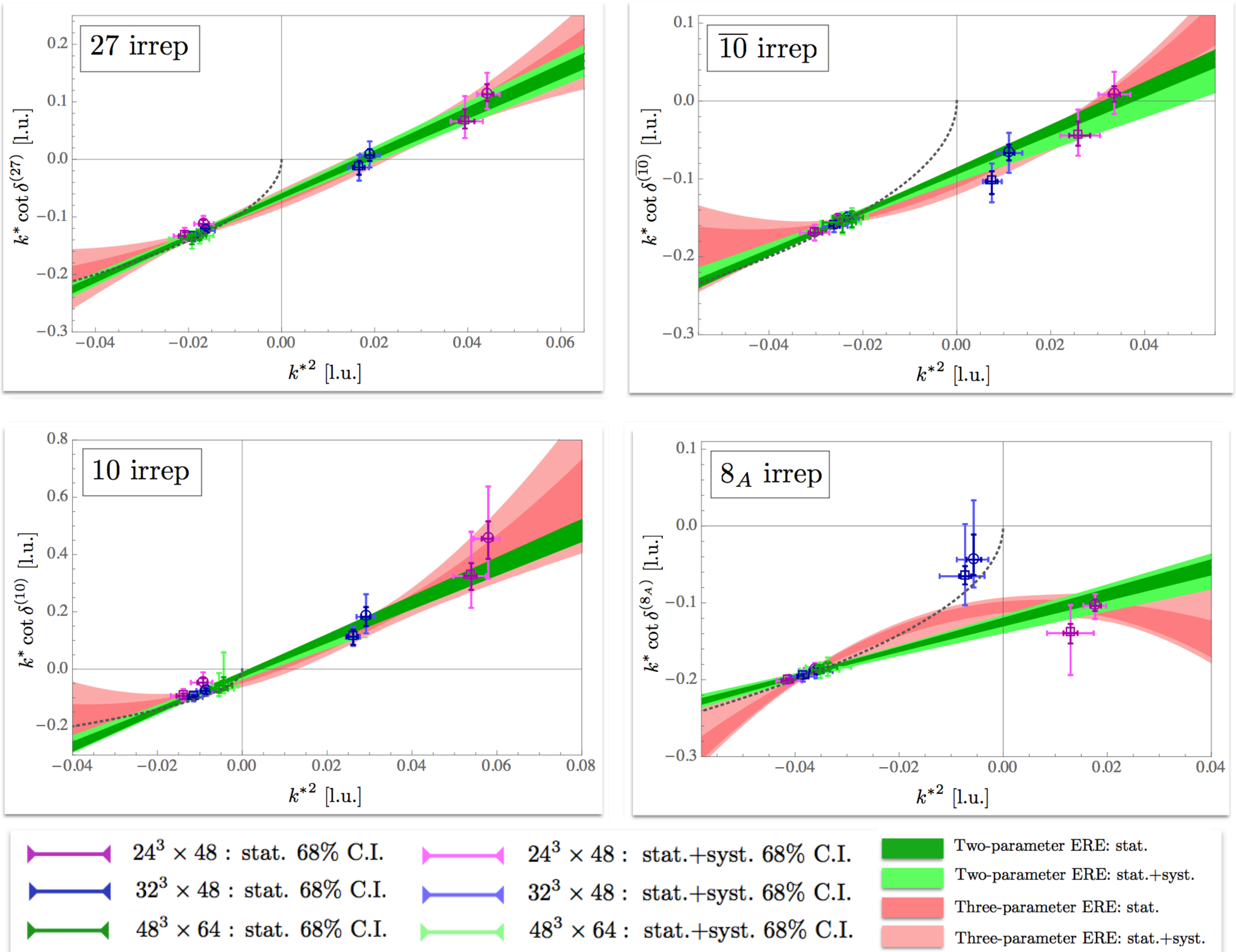

27 irrep
$\overline{10}$ irrep
10 irrep
8_A irrep
$k^* \cot\delta^{(27)}$ [l.u.]
$k^* \cot\delta^{(\overline{10})}$ [l.u.]
$k^* \cot\delta^{(10)}$ [l.u.]
$k^* \cot\delta^{(8_A)}$ [l.u.]
k^{*2} [l.u.]
$24^3 \times 48$: stat. 68% C.I.
$32^3 \times 48$: stat. 68% C.I.
$48^3 \times 64$: stat. 68% C.I.
$24^3 \times 48$: stat.+syst. 68% C.I.
$32^3 \times 48$: stat.+syst. 68% C.I.
$48^3 \times 64$: stat.+syst. 68% C.I.
Two-parameter ERE: stat.
Two-parameter ERE: stat.+syst.
Three-parameter ERE: stat.
Three-parameter ERE: stat.+syst.

ERE results

Scattering lengths in all channels are unnaturally large compared to effective range, although less so than nucleon-nucleon systems in nature

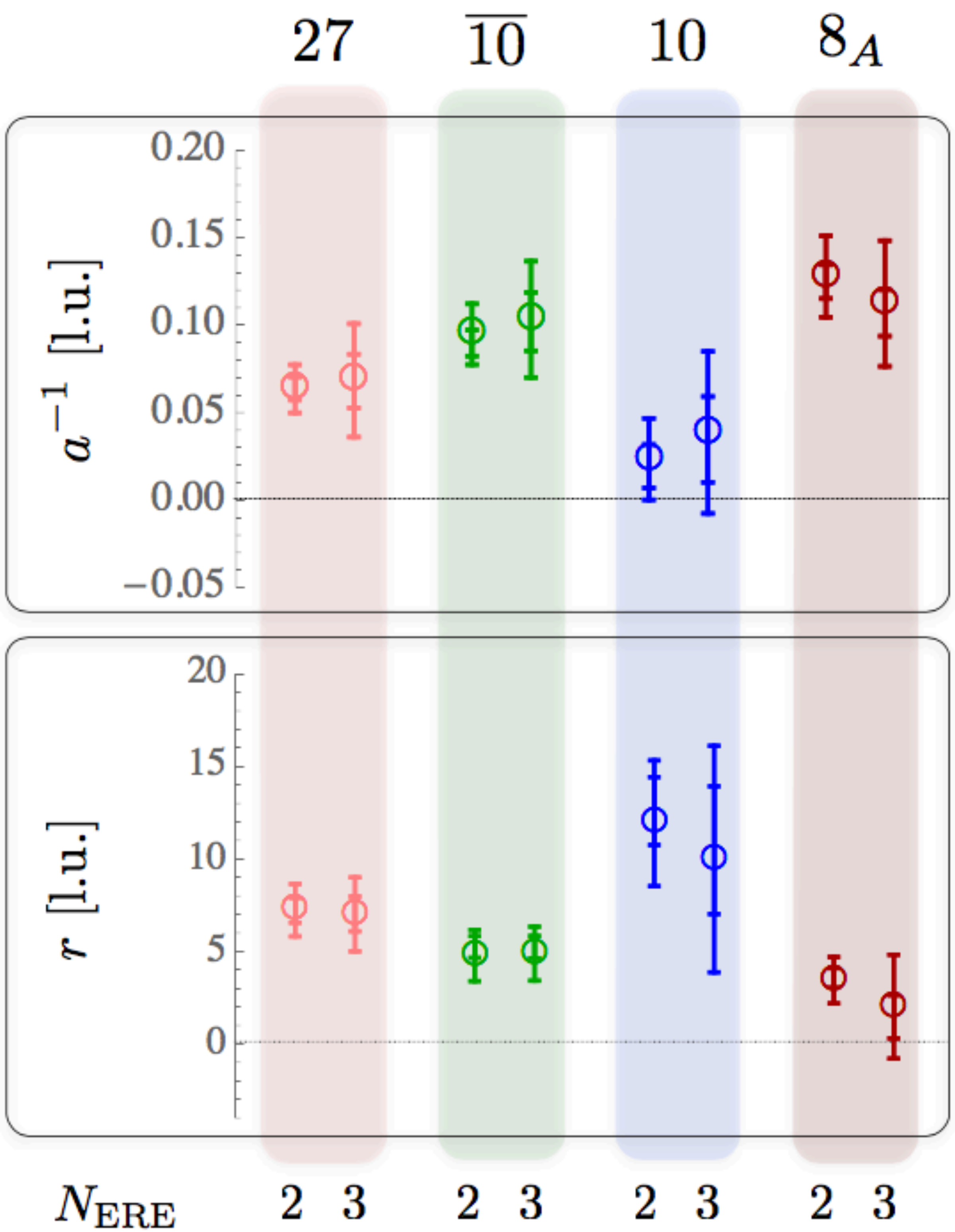

$$m_\pi \sim 800 \text{ MeV}$$

$$(r/a)_{27} = 0.459(75) \qquad (r/a)_{\overline{10}} = 0.452(71)$$

$$(r/a)_{10} = 0.28(25) \qquad (r/a)_{8_A} = 0.439(90)$$

$$m_\pi \sim 140 \text{ MeV}$$

$$(r/a)_{NN(^1S_0)} \approx 0.32 \qquad (r/a)_{NN(^3S_1)} \approx -0.14$$

Note uncertainties on scattering length and effective range highly correlated

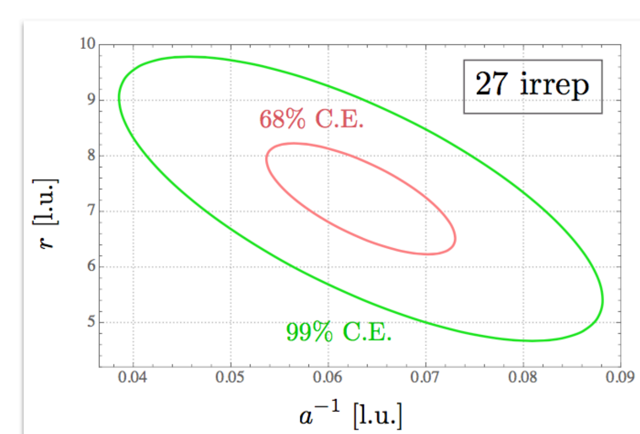

Binding energies

ERE parameterization can be used to look for poles in scattering amplitude corresponding to baryon-baryon bound states,

$$[k^* \cot \delta(k*)|_{k^*=i\kappa} + \kappa = 0$$

More precise constraints found by directly fitting finite-volume energy levels to (truncated expansion of) Lüscher quantization condition

$$|k^*(L)| = \kappa + \frac{Z^2}{L}\left[6e^{-\kappa L} + \frac{12}{\sqrt{2}}e^{-\sqrt{2}\kappa L} + \frac{8}{\sqrt{3}}e^{-\sqrt{3}\kappa L} + \ldots\right]$$

$\lesssim 10^{-3}$

Binding energy results:

$B_{27} = 20.6(3.3)$ MeV

$B_{\overline{10}} = 27.9(3.8)$ MeV

$B_{10} = 6.7(6.5)$ MeV

$B_{8_A} = 40.7(3.5)$ MeV

Consistent with bound or unbound

Survey of LQCD studies

Several groups have studied NN interactions with $m_\pi \sim 800 \text{ MeV}$

HAL QCD results (HAL QCD method) prefer unbound deuteron and dineutron

Aoki et al, Comput. Sci. Dis. 1 (2008)
Iritani et al, JHEP 1610 (2016)
HAL QCD, PRD 99 (2019)
HAL QCD, Nucl. Phys. A881 (2012)
Iritani et al, PRD 96 (2017)
HAL QCD, JHEP 1903 (2019)

PACS results (Lüscher methods) prefer bound deuteron and dineutron

PACS-CS, PRD 81 (2010)
PACS, Lattice 2017

NPLQCD results (Lüscher methods) prefer bound deuteron and dineutron

NPLQCD, PRD 87 (2013)
NPLQCD, PRD 96 (2017)

CalLatt results (Lüscher methods) prefer bound deuteron and dineturon

Berkowitz et al, Phys. Lett. B 285 (2017)

Mainz results (Lüscher methods) prefer unbound dineutron

Francis et al, PRD 99 (2019)

More work needed to understand discrepancies

Low-energy Lagrangian

With $SU(3)$ flavor symmetry, baryon octet organized as

$$B = \begin{pmatrix} \frac{\Sigma^0}{\sqrt{2}} + \frac{\Lambda}{\sqrt{6}} & \Sigma^+ & p \\ \Sigma^- & -\frac{\Sigma^0}{\sqrt{2}} + \frac{\Lambda}{\sqrt{6}} & n \\ \Xi^- & \Xi^0 & -\sqrt{\frac{2}{3}}\Lambda \end{pmatrix} = B_i t_i$$

Low-energy effective Lagrangian for non-relativistic baryons with $p \ll m_\pi$:

$$\mathcal{L}_{BB}^{(6)} = -c_1 \mathrm{Tr}(B_i^\dagger B_i B_j^\dagger B_j) - c_2 \mathrm{Tr}(B_i^\dagger B_j B_j^\dagger B_i) - c_3 \mathrm{Tr}(B_i^\dagger B_j^\dagger B_i B_j)$$
$$-c_4 \mathrm{Tr}(B_i^\dagger B_j^\dagger B_j B_i) - c_5 \mathrm{Tr}(B_i^\dagger B_i)\mathrm{Tr}(B_j^\dagger B_j) - c_6 \mathrm{Tr}(B_i^\dagger B_j)\mathrm{Tr}(B_j^\dagger B_i)$$

Savage, Wise, PRD 53 (1993)

In large N_c limit, effective Lagrangian further simplifies due to $SU(6)$ analog of Wigner symmetry arising from large N_c quark spin-flavor symmetry

Kaplan, Savage, Phys. Lett. B365 (1996)

$$\mathcal{L}_{BB}^{(6)} = -a(\Psi_{\mu\nu\rho}^\dagger \Psi^{\mu\nu\rho})^2 - b\Psi_{\mu\nu\sigma}^\dagger \Psi^{\mu\nu\tau} \Psi_{\rho\delta\tau}^\dagger \Psi^{\rho\delta\sigma}$$

$SU(6)$ spin-flavor index

$$\Psi^{(\alpha r)(\beta s)(\gamma t)} = T_{\alpha\beta\gamma}^{ijk} + \frac{1}{\sqrt{18}} \left(B_{u,\alpha}^r \varepsilon^{ust} \varepsilon_{\beta\gamma} + B_{u,\beta}^s \varepsilon^{utr} \varepsilon_{\gamma\alpha} + B_{u,\gamma}^t \varepsilon^{urs} \varepsilon_{\alpha\beta} \right)$$

Pionless effective field theory

EFT specified by $\mathcal{L}^{(6)}_{BB}$ and choice of power counting $a^{-1} = \infty$ $a^{-1} = 0$

Two renormalization group fixed points to call LO: free-field and unitary Fermi gas

Scattering lengths prefer unitary Fermi gas, both in nature at with $m_\pi \sim 800$ MeV

KSW power counting — operators in $\mathcal{L}^{(6)}_{BB}$ nonperturbative

Kaplan, Savage, Wise, Phys. Lett. B424 (1998) van Kolck, Nucl. Phys. A645 (1999)

$\mathcal{A}_{LO} =$ 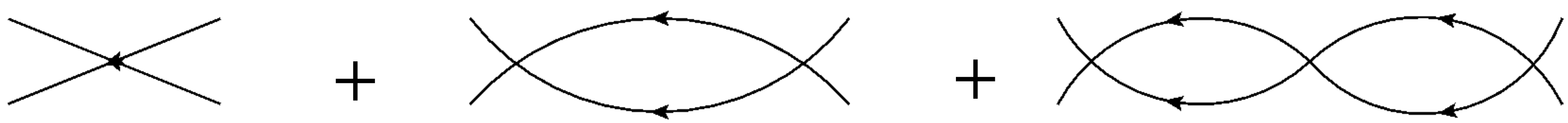 $+ \ldots$

Summing geometric series of bubble diagrams gives

$$\left[-\frac{1}{a^{(27)}} + \mu\right]^{-1} = \frac{M_B}{2\pi}\left(a - \frac{b}{27}\right) + \mathcal{O}\left(\frac{1}{N_c^2}\right), \quad \left[-\frac{1}{a^{(\overline{10})}} + \mu\right]^{-1} = \frac{M_B}{2\pi}\left(a - \frac{b}{27}\right) + \mathcal{O}\left(\frac{1}{N_c^2}\right),$$

$$\left[-\frac{1}{a^{(10)}} + \mu\right]^{-1} = \frac{M_B}{2\pi}\left(a + \frac{7b}{27}\right) + \mathcal{O}\left(\frac{1}{N_c}\right), \quad \left[-\frac{1}{a^{(8_A)}} + \mu\right]^{-1} = \frac{M_B}{2\pi}\left(a + \frac{b}{27}\right) + \mathcal{O}\left(\frac{1}{N_c}\right),$$

$$\left[-\frac{1}{a^{(8_S)}} + \mu\right]^{-1} = \frac{M_B}{2\pi}\left(a + \frac{b}{3}\right) + \mathcal{O}\left(\frac{1}{N_c}\right), \quad \left[-\frac{1}{a^{(1)}} + \mu\right]^{-1} = \frac{M_B}{2\pi}\left(a - \frac{b}{3}\right) + \mathcal{O}\left(\frac{1}{N_c}\right),$$

Emergent $SU(6)$ symmetry

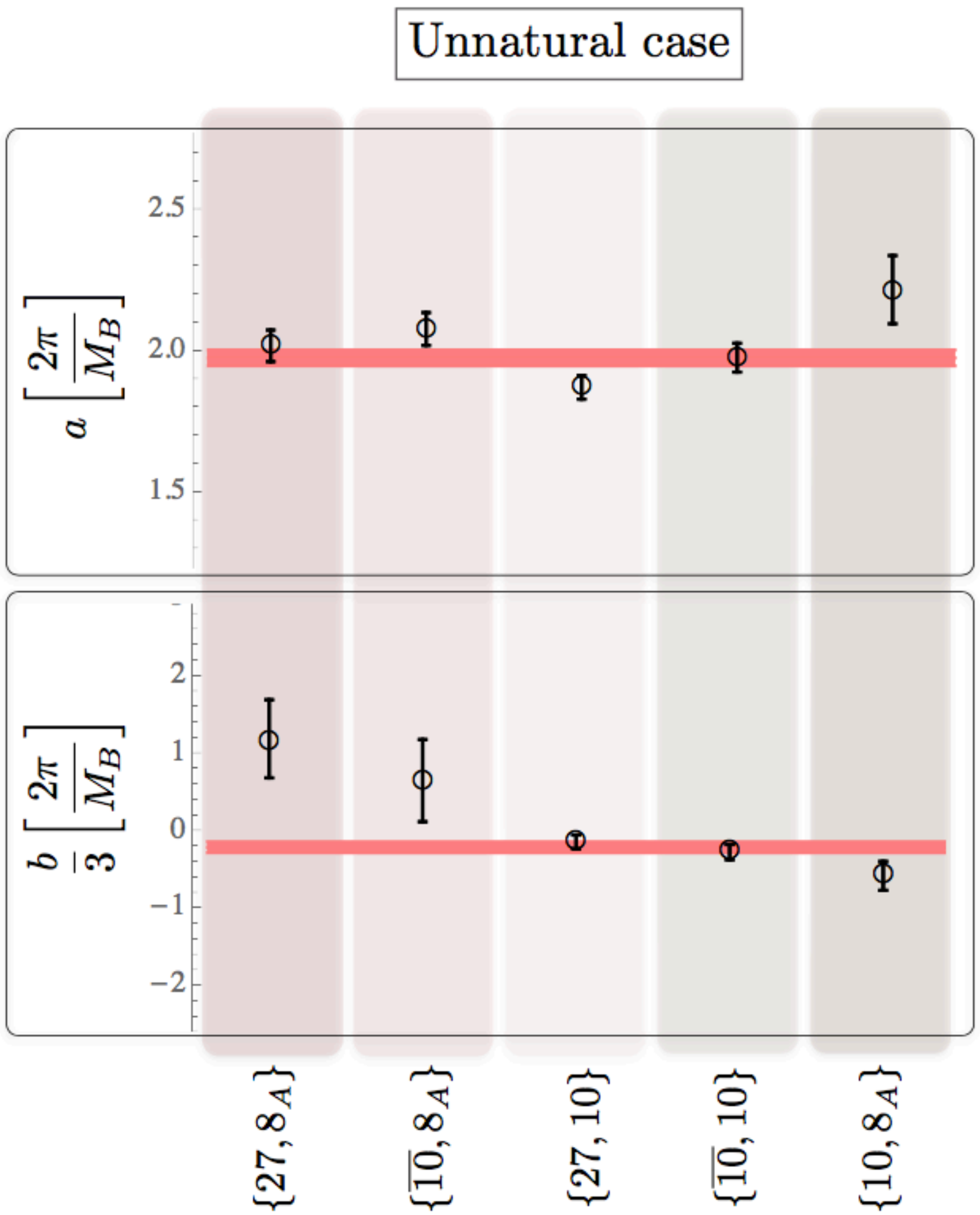

$SU(6)$ - symmetric couplings can be fit from LQCD results to any two channels (or all 4, pink band)

Consistency: 4 channels described by 2 couplings

$SU(6)$ predicted by large N_c emerges!

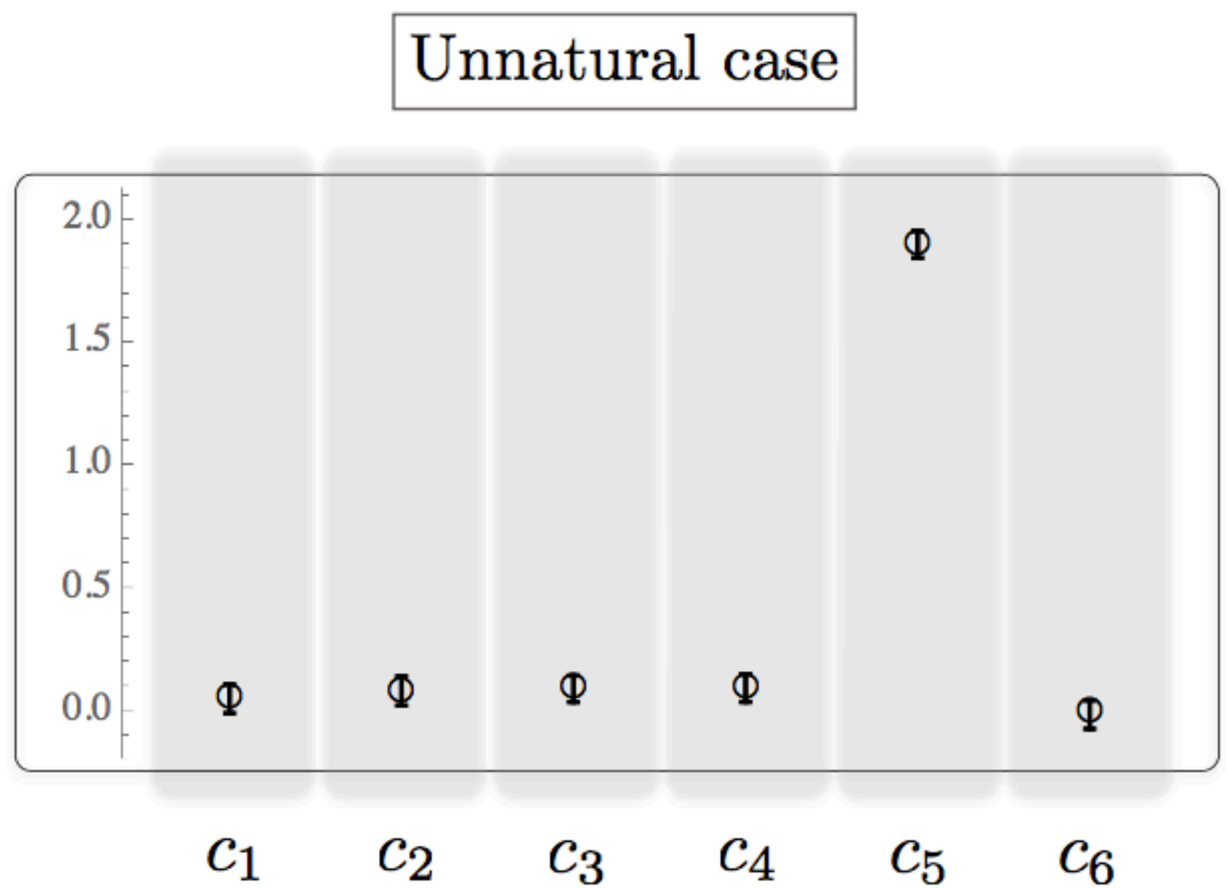

Assuming $SU(6)$, scattering lengths predicted for 8_S and 1, all 6 $SU(3)$ couplings can be extracted

Only c_5 (only a) resolved from 0

Emergent $SU(16)$ symmetry

LQCD results for all 4 channels described by one-parameter EFT with baryons in fundamental representation of $SU(16)$ spin-flavor symmetry

$$\mathcal{B} = (p_\uparrow, n_\uparrow, \Sigma^+_\uparrow, \Sigma^0_\uparrow, \Lambda_\uparrow, \Sigma^-_\uparrow, \Xi^-_\uparrow, \Xi^0_\uparrow, p_\downarrow, n_\downarrow, \Sigma^+_\downarrow, \Sigma^0_\downarrow, \Lambda_\downarrow, \Sigma^-_\downarrow, \Xi^-_\downarrow, \Xi^0_\downarrow)$$

$$\mathcal{L}^{(6)}_{BB} = -c_5 (\mathcal{B}^\dagger_A \mathcal{B}_A)(\mathcal{B}^\dagger_B \mathcal{B}_B)$$

Who ordered that?

Emergent $SU(16)$ symmetry

LQCD results for all 4 channels described by one-parameter EFT with baryons in fundamental representation of $SU(16)$ spin-flavor symmetry

$$\mathcal{B} = (p_\uparrow, n_\uparrow, \Sigma^+_\uparrow, \Sigma^0_\uparrow, \Lambda_\uparrow, \Sigma^-_\uparrow, \Xi^-_\uparrow, \Xi^0_\uparrow, p_\downarrow, n_\downarrow, \Sigma^+_\downarrow, \Sigma^0_\downarrow, \Lambda_\downarrow, \Sigma^-_\downarrow, \Xi^-_\downarrow, \Xi^0_\downarrow)$$

$$\mathcal{L}^{(6)}_{BB} = -c_5(\mathcal{B}^\dagger_A \mathcal{B}_A)(\mathcal{B}^\dagger_B \mathcal{B}_B)$$

Who ordered that?

New conjectured principle — "dynamical entanglement suppression"

Beane, Kaplan, Klco, Savage, PRL 122 (2019)

EFT parameters values with enhanced symmetry also minimize entanglement produced when time-evolving two-baryon systems

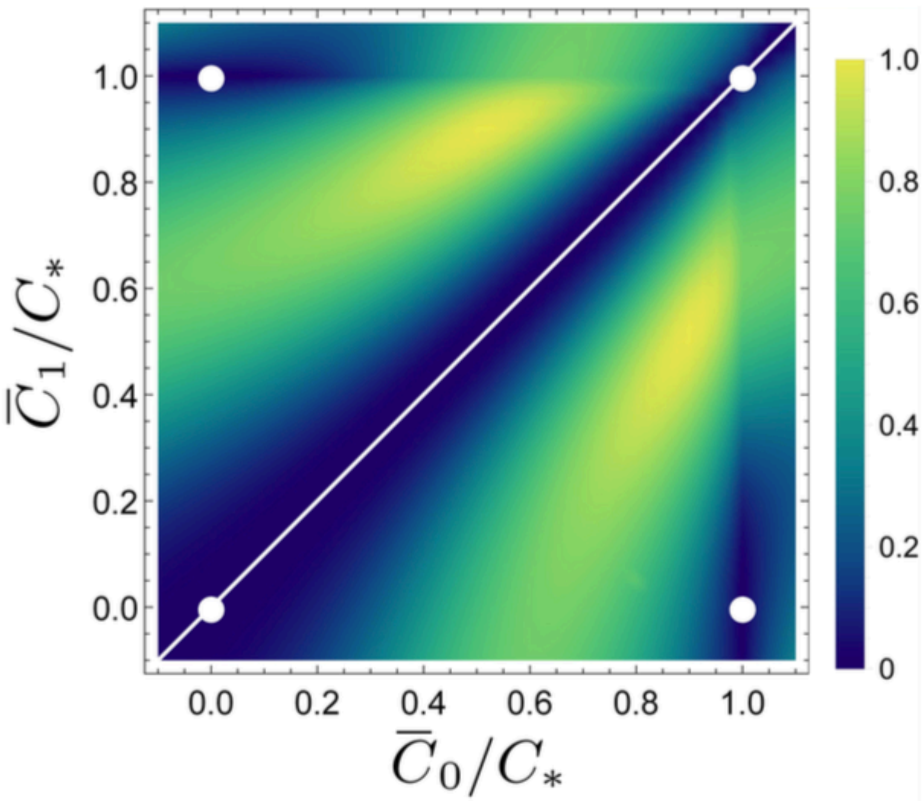

Beane, Kaplan, Klco, Savage, PRL 122 (2019)

Outlook

Electroweak reactions and quark/gluon structure of nuclei at $m_\pi \sim 800\ \mathrm{MeV}$

NPLQCD, PRL 119 (2017a)   NPLQCD, PRL 119 (2017b)   NPLQCD, PRD 96 (2017)   NPLQCD, PRL 120 (2018)

Does approximate $SU(16)$ symmetry exist in nature? Is entanglement suppression the principle behind its emergence?

Calculations at lighter quark masses performed by NPLQCD, noisier data requires careful multi-state analysis. Results coming soon to arXiv near you

— with Assumpta Parreño and graduate student Marc Illa

Exploratory calculation at nearly physical quark masses underway — stay tuned!